



Norwegian University of
Science and Technology

Numerical Investigation of a Phase Change Materials (PCM) heat exchanger

For small scale combustion appliances.

Jerol Soibam

Master's Thesis

Submission date: October 2017

Supervisor: Nils Erland L Haugen, EPT

Norwegian University of Science and Technology
Department of Energy and Process Engineering

Numerical Investigation of a heat exchanger using phase change materials (PCMs)

For small-scale combustion appliances

By

JEROL SOIBAM



Norwegian University of
Science and Technology

Department of Energy and Process Engineering
NTNU

Master Thesis

October 2017

Internal supervisor:

Nils Erland L. Haugen
Associate Professor
Department of Energy and Process Engineering
NTNU

External supervisors:

Alexis Sevault
PhD, Research Scientist
SINTEF Energy Research

EPT-M-2017-124

MASTER THESIS

for

Student: Jerol Soibam

Spring 2017

Numerical investigation of innovative thermal energy storage solutions for wood stoves based on phase change materials (PCM)***Numerisk studie om innovative løsninger til termisk energilagring basert på faseendringsmaterialer (PCM)*****Background and objective**

The topic of the Master Thesis has been raised by the research project PCM-Eff (<https://www.sintef.no/en/projects/pcm-eff/>), coordinated by SINTEF Energy Research, aiming at building advanced knowledge on the application of phase change materials (PCM) and their integration in various thermal processes.

The focus of PCM-Eff is on latent heat storage, based on heat absorption (or release) when a storage material undergoes a phase change, usually from solid to liquid (or liquid to solid). Though many PCM materials are well documented in the literature, their implementation is still limited due to the complexity of designing suitable interfaces between PCM, heat source and heat sink.

The purpose of the present study is to carry out a computational fluid dynamic (CFD) investigation of innovative designs of thermal energy storage solutions based on PCM for biomass-based residential heating appliances. The task on numerical simulation will be initiated before the student starts, with Modelica/Dymola and Fluent. The student's task will consist in further developing the numerical investigation and help solve the key issues related to the modelling of the solid/liquid boundary of the phase change material. The student will also contribute in optimizing the design and heat transfer conditions through innovative ideas. Different design configurations should be compared quantitatively to issue recommendations.

The work will be performed in collaboration with several research scientists from SINTEF Energy Research with a strong background in numerical simulations and industrial thermal processes. The student will participate to the monthly team meetings with the whole project team to follow up on the general progress and get more familiar with the research project. The student may participate in the writing of a peer-reviewed scientific journal paper based on the results of the study.

The following tasks are to be considered:

1. Literature study on phase change materials and their applications
2. Numerical (CFD) simulations using ANSYS Fluent
3. Quantitative analysis of the CFD results
4. Contribution to improved design through recommendations

-- " --

Within 14 days of receiving the written text on the master thesis, the candidate shall submit a research plan for his project to the department.

When the thesis is evaluated, emphasis is put on processing of the results, and that they are presented in tabular and/or graphic form in a clear manner, and that they are analyzed carefully.

The thesis should be formulated as a research report with summary both in English and Norwegian, conclusion, literature references, table of contents etc. During the preparation of the text, the candidate should make an effort to produce a well-structured and easily readable report. In order to ease the evaluation of the thesis, it is important that the cross-references are correct. In the making of the report, strong emphasis should be placed on both a thorough discussion of the results and an orderly presentation.

The candidate is requested to initiate and keep close contact with his/her academic supervisor(s) throughout the working period. The candidate must follow the rules and regulations of NTNU as well as passive directions given by the Department of Energy and Process Engineering.

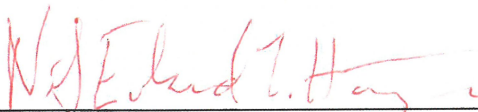
Risk assessment of the candidate's work shall be carried out according to the department's procedures. The risk assessment must be documented and included as part of the final report. Events related to the candidate's work adversely affecting the health, safety or security, must be documented and included as part of the final report. If the documentation on risk assessment represents a large number of pages, the full version is to be submitted electronically to the supervisor and an excerpt is included in the report.

Pursuant to "Regulations concerning the supplementary provisions to the technology study program/Master of Science" at NTNU §20, the Department reserves the permission to utilize all the results and data for teaching and research purposes as well as in future publications.

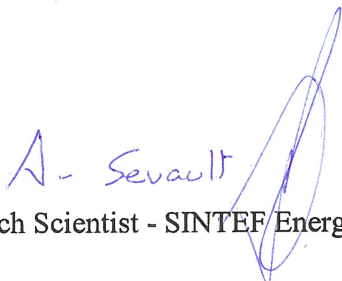
The final report is to be submitted digitally in DAIM. An executive summary of the thesis including title, student's name, supervisor's name, year, department name, and NTNU's logo and name, shall be submitted to the department as a separate pdf file. Based on an agreement with the supervisor, the final report and other material and documents may be given to the supervisor in digital format.

- Work to be done in lab (Water power lab, Fluids engineering lab, Thermal engineering lab)
 Field work

Department of Energy and Process Engineering, 1 of June 2017



Nils Erland Haugen
Academic Supervisor

Research Advisor: 
Alexis Sevault (PhD Research Scientist - SINTEF Energy Research)

Acknowledgments

The internship thesis opportunity I had with SINTEF Energy and NTNU, Norway was an excellent way to learn and aid in professional development. I am so grateful to have met wonderful people and recognized professionals, who led me through this internship period.

First and foremost, I would like to thank my advisor, Alexis Sevault, PhD, Research Scientist, SINTEF Energy, with profound gratitude. He has been supportive since the days I began my internship. Alexis has supported me not only by providing me this internship but also with guidance to get around the new city and always encouraging me through the rough road to finish this thesis. Thanks to him I got to learn lots of valuable lessons of life, and also I had the opportunity to learn about PCMs and how I can implement this study in my upcoming career. I would also like to thank him for involving me as a part of the PCM-Eff project, SINTEF Energy AS, which gave me a wider exposure. And during the most difficult times when writing and analyzing the result of this thesis, he gave me the moral support and freedom I needed to move on.

I would like to thank my second advisor Nils Erland L. Haugen Associate Professor, NTNU, with sincere gratitude. He has been very supportive throughout the completion of this thesis and helped me with all the questions related to my thesis. Every time, I come out after a discussion with him it always showed me different ways to approach the problem with better clarity. I would like to thank Nils again for providing me with the necessary resources through NTNU to make this thesis possible.

I would also like to thank the project members of PCM-Eff, for their support and valuable comments.

I would also like to thank Arpit Singhal, PhD candidate at NTNU for giving me advice on how to approach the problems, through his busy schedule. I would also like to thank Martin Thalfeldt, Post-doc, NTNU for his great help for letting me run most of my simulation on his computer. It would not have been possible to obtain this simulation result without his support.

Finally, I would like to thank my parents and siblings for providing me with unfailing support and continuous encouragement throughout my years of study and through the process of this internship and writing this thesis.

Abstract

Thermal energy stored in concentrated wood stovepipe can improve the dispatchability and eliminates the miss-match between the energy supply and demand for heating the room. For this purpose, phase change materials are particularly attractive since they provide a high-energy storage density at a constant temperature which corresponds to the phase transition temperature of the material.

In this thesis report, the numerical investigation is performed to evaluate the heat transfer rate, melting rate, solidification rate of the PCM (erythritol) and temperature distribution from the PCM in a stovepipe to the surrounding. To enhance the heat transfer inside the PCM, fins were implemented on the inner pipe wall. Two models were developed for vertical wood stovepipe one with constant wall temperature and another with hot gas flowing in the inner pipe which would serve as the heat generator for the PCM. These models were design and mesh in ANSYS Workbench, and CFD simulation was carried out in ANSYS FLUENT 17.2, and the simulation results were analyzed using Tecplot 360 Ex.

The effects of frequencies of fins in the PCM block was studied, and the computational results showed that having 3 fins for 300 mm pipe was the best solution. The effect of fins lengths cases was also analyzed and compared with no fin case. It showed that having fin lengths of 17.5 mm, 35 mm, 52.5 mm and 70 mm fins were 57.8 %, 63.2 %, 68.4 % and 73.6 % faster than without fins for melting 90 % of PCM volume. Further observation was made on heat inputted to the PCM and heat given out of the outer pipe to the surrounding for all the cases, and it showed that 35 mm finned case was the most reliable system for both the models in our case.

Nomenclature

λ	Latent heat of fusion ($J.kg^{-1}$)
β	Liquid fraction
Δs	Wall distance (mm)
ϵ	Kinetic dissipation rate (m^2s^{-3})
μ	Dynamic viscosity ($kg\ m^{-1}s$)
ρ	Density($kg\ m^{-3}$)
C	Mushy zone constant ($kg\ m^{-3}s^{-1}$)
c_{eff}	Effective heat capacity ($J(K\ kg)^{-1}$)
c_p	Specific heat capacity at constant pressure ($J.(kg.K)^{-1}$)
D_h	Hydraulic diameter (m)
dT	Change in temperature
g	Gravity acceleration (ms^{-2})
H	Specific enthalpy ($J.kg^{-1}$)
h	Sensible enthalpy ($kJ\ kg^{-1}$)
h_{ref}	Reference enthalpy in reference temperature T_{ref} ($kJ\ kg^{-1}$)
k	Kinetic energy (m^2s^{-2})
k	Thermal conductivity (W/mK)
k_l	PCM liquid state thermal conductivity (W/mK)
k_s	PCM solid state thermal conductivity (W/mK)
L	Latent heat (J)
Q	Heat transfer rate (W)
$Re_{D,crit}$	Critical Reynolds number
Re_D	Reynolds number
S	Momentum source term(Pa/m)
T	Temperature (K)

t	Time (s)
T_f	Final temperature (K)
T_i	Initial temperature (K)
T_l	PCM liquid temperature (K)
T_s	PCM solid temperature (K)
u	Velocity in x direction (m/s)
v	Velocity in y direction (m/s)
CFD	Computational fluid dynamics
CNF	Carbon nanofibre
CNT	Carbon nanotubes
FCC	Face-centered cubic
HP	Heat pipe
HTF	Heat transfer fluid
LHS	Latent heat storage
LHTES	Latent heat thermal energy storage
NW	Nanowires
PCM	Phase change materials
SHS	Sensible heat storage

List of Figures

1	<i>Phase change diagram: temperature as a function of heat added. T_m and T_e indicates the melting and evaporation temperature, respectively.</i>	14
2	<i>Classification of Phase change Materials (PCMs)</i>	17
3	<i>Techniques for heat transfer enhancement of LHTES system.</i>	24
4	<i>General types of fins</i>	25
5	<i>Cascaded configuration of LHTES system during charging and discharging.[36]</i>	25
6	<i>Schematic of multiple PCMs in shell-and tube LHTES unit</i>	26
7	<i>Arrangements of carbon fibers in cylindrical capsules [32]</i>	28
8	<i>Graphical representation of effective heat capacity method.</i>	29
9	<i>Graphical representation of the enthalpy formulation method.</i>	30
10	<i>Effect of C values (10^4 and 10^5) on melting process after 10 min.</i>	33
11	<i>Effect of C values (10^6 and 10^7) on melting process after 10 min.</i>	34
12	<i>Effect of convection on PCM melting process after 15 min.</i>	34
13	<i>wood stove pipe and fins</i>	37
14	<i>Top view of the wood stove pipe</i>	38
15	<i>Enhanced thermal conductivity calculation table</i>	39
16	<i>2D axisymmetric mesh geometry</i>	39
17	<i>2D axisymmetric constant wall temperature and hot gas inlet temperature models</i>	40
18	<i>Effect of fin frequency on melting and solidification processes.</i>	46
19	<i>CFD results of melting rate due to fin frequency for 35mm fins after one hour.</i>	47
20	<i>CFD results of solidification rate due to fin frequency for 35mm fin after one hour.</i>	47
21	<i>Effect of fin length on melting and solidification process.</i>	48
22	<i>CFD results of fin length on melting process after one hour.</i>	49
23	<i>CFD results of fin length on solidification process after one hour.</i>	49
24	<i>Effect of fin length on melting and solidification processes for hot gas inlet with 498 K.</i>	50
25	<i>Effect of fin length on melting and solidification processes for hot gas inlet with 498 K for dynamic case.</i>	51
26	<i>CFD results for melting after one hour for different cases with hot.</i>	51
27	<i>CFD results for solidification after one hour for different cases with hot gas.</i>	52
28	<i>Variation of temperature on out pipe-wall during charging and discharging of PCM</i>	53
29	<i>CFD results for variation of temperature in heat exchanger during melting process after one hour.</i>	54
30	<i>CFD results for variation of temperature in heat exchanger during solidification process after an hour.</i>	54
31	<i>Variation of temperature on out pipe-wall during charging and discharging for hot gas</i>	55

32	<i>CFD temperature profile for different fin cases for melting process after one hour with hot gas at 498 K.</i>	56
33	<i>CFD temperature profile for different fin cases for solidification process after one hour with inlet and outlet as adiabatic walls.</i>	56
34	<i>Variation of heat supplied to the PCM and the outpipe.</i>	57
35	<i>variation of temperature in PCM during charging and discharging . . .</i>	58

List of Tables

1	<i>Thermal properties of alkanes.</i>	18
2	<i>Thermal properties of some common fatty acids.</i> [14]	19
3	<i>Thermal properties of solid-solid phase transition for polyalcohols and amine derivatives [18-19].</i>	19
4	<i>Thermal properties of some salt hydrates.</i>	20
5	<i>Thermal properties of metallic compounds</i>	20
6	<i>Thermal properties of Eutectics materials.</i>	21
7	<i>Properties of common fin materials.</i>	24
8	<i>Fin length in LHTEs system.</i>	40
9	<i>Fin frequency in LHTEs system.</i>	40
10	<i>Setup for FLUENT simulation.</i>	41
11	<i>Thermophysical properties of erythritol PCM.</i>	42

Contents

1	Introduction	13
1.1	Background	13
1.2	Objectives	13
2	Theoretical background	14
2.1	Thermal energy storage	14
2.1.1	Sensible heat storage	14
2.1.2	Latent heat storage	15
2.2	PCM Selection	16
2.3	Classification of PCMs	16
2.3.1	Organic PCM	17
2.3.2	Inorganic PCM	19
2.3.3	Eutectics	21
2.4	PCM applications	21
2.4.1	Low temperature	21
2.4.2	High temperature	23
3	Heat transfer in phase change materials	23
3.1	Latent heat TES design challenges	23
3.2	Heat transfer enhancement	24
3.3	Application of heat pipes	25
3.4	Multiple PCMs	26
3.5	Effect of porous materials	26
3.6	Dispersion of nanoparticles	27
3.7	Dispersion of low density materials	27
4	Mathematical and numerical modeling of LHTES system	28
4.1	Moving boundary problems	28
4.2	Effective heat capacity method	29
4.3	Enthalpy formulation method	30
4.4	Governing equations used in ANSYS Fluent	31
4.5	Effect of mushy zone constant	33
4.6	Numerical solution with conduction and convection	34
5	Modeling methods	37
5.1	Geometry specification	37
5.1.1	Fins in hot gas domain	38
5.1.2	Mesh specification	38
5.2	Types of model	40
5.3	Computational methodology	41
5.3.1	Initial and boundary conditions	42
5.3.2	Parameters for converged solution	43
5.4	Determination of flow model	44

6	Results and discussion	46
6.1	Effect of fin frequency on melting and solidification processes	46
6.2	Effect of fin lengths on melting and solidification processes	47
6.2.1	Constant wall temperature	48
6.2.2	Hot gas flowing in the stovepipe with an inlet temperature of 498 K	49
6.3	Temperature variation on the outer pipe wall	52
6.3.1	Constant wall temperature	52
6.3.2	Hot gas flowing in the stovepipe with an inlet temperature of 498K	54
6.4	Heat given to the PCM and heat transfer to the outer pipe	56
6.5	Variation of temperature in PCM during charging and discharging . .	57
7	Conclusion and recommendations	59

1 Introduction

1.1 Background

The continuous increase in greenhouse gas emissions and volatility of fuel price make it important for us to adapt to renewable energy and use energy more effectively. One of the options to use the renewable energy more efficiently is to develop energy storage devices. Allowing the energy to be stored in the suitable form, which can be extracted later in the desired form depending on the usability. Energy storage not only reduces the mismatch between supply and demand but also improves the performance and reliability of energy systems and plays an important role in conserving the energy [4]. The different forms of energy that can be stored are chemical, mechanical, electrical and thermal. However, in this case, we will focus only on thermal energy storage and it will be discussed in the context of latent heat. One of the prospective techniques of storing thermal energy (latent heat) is the application of phase change materials (PCMs).

In Norway, power consumption is increasing, while the power production is stagnating [3]. A large part of this power is being used for residential heating. Therefore, an alternative method such as biomass heating (wood stove) has to be employed to keep the houses warm. The current goal of the country is to double the use of bio-energy between 2008 and 2020. Modern wood stoves have a thermal efficiency of 70 to 80 % at normal load and produce more heat than what is actually required to heat up the house. There is an excessive heat that is released to the surrounding from the stove pipe of the wood stove. Hence, it becomes essential to absorb this excessive heat and supply it to the surrounding when it is needed i.e when the wood stove is off. This process would be possible if we had a phase changing material (PCM) wrapped around the hot exhaust pipe. The advantage of using a PCM is that the material can store a large amount of heat by melting and solidification processes. When heat is added to the PCM its temperature remains constant at melting temperature of PCM until the whole PCM is melted, as heat stored is in the form of latent heat.

1.2 Objectives

This work mainly focuses on the investigation of heat storage in a PCM, solidification & melting of the PCM and heat release to the surrounding from the storage unit. As the conductivity of PCMs is generally low, fins have been attached to the surface of the pipe to improve the heat transfer in the PCMs. Different lengths, thicknesses, and frequencies of the fins on the pipe are also studied to better understand the behavior of the system. An initial case study is performed considering that a constant temperature is maintained in the inner pipe for the melting and solidification process. To make the problem closer to reality, hot gas was introduced into the inner pipe as a mode of heat generator. The goal of this study is to understand how much heat is stored in the PCM and how much heat it can supply to the surrounding. These numerical simulations are performed using ANSYS FLUENT

17.2.

2 Theoretical background

Thermal energy can be stored as a change in internal energy of a material as sensible heat, latent heat and thermochemical or combination of these. Phase change material has the capability to store a large quantity of heat in a relatively small mass and volume with small change in temperature. In this chapter, we will discuss the basic of thermal energy storage (TES), PCM working principle, characteristic and its applications.

2.1 Thermal energy storage

Thermal energy can be stored using different physical or chemical processes, and each method has different characteristics. The heat stored due to change in temperature of any substance is called sensible heat. The ratio between the stored heat and the temperature difference is defined as the heat capacity. The easiest way to indicate and measure is by using a sensor like a thermometer. Heat can also be stored as latent heat i.e.the amount of heat absorbed or released during a phase change.

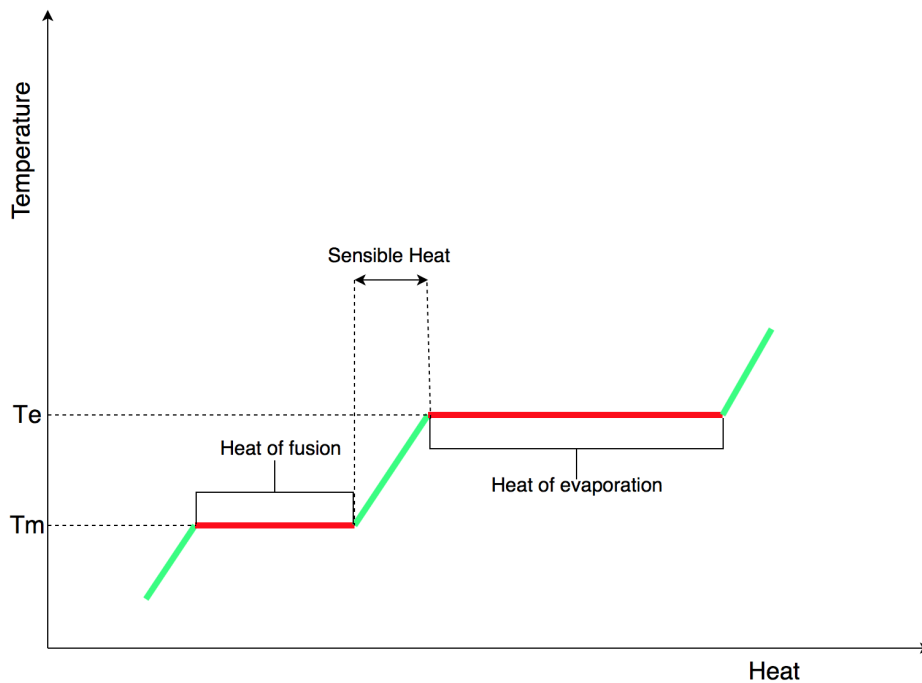


Figure 1: Phase change diagram: temperature as a function of heat added. T_m and T_e indicates the melting and evaporation temperature, respectively.

2.1.1 Sensible heat storage

With sensible heat storage (SHS), thermal energy is stored by raising the temperature of a solid or liquid or gas. SHS system utilizes the heat capacity and the change

in temperature of the material during the process of charging and discharging. The amount of heat stored depends on the specific heat of the medium, the temperature change and the amount of storage material.

$$Q = \int_{T_i}^{T_f} mc_p dT = mc_p(T_f - T_i) \quad (1)$$

2.1.2 Latent heat storage

Latent heat storage (LHS) is based on the heat absorption or release when a storage material undergoes a phase change from solid to liquid or liquid to gas or vice versa. LHS is attractive topic since it provides a high-energy storage density and has the capacity to store energy at a constant temperature or over a limited range of temperature variation, which is the temperature that corresponds to the phase transition temperature of the material [5]. The storage capacity of the LHS system with a PCM medium [4] is given by:

$$Q = \int_{T_i}^{T_f} mc_p dT + ma_m \Delta h_m + \int_{T_i}^{T_f} mc_p dT \quad (2)$$

There are three possible types of phase change [9] :

- Solid-Liquid: This phase change is an isothermal process, and usually there is a small volume difference between the two phases. Figure 1 clearly shows the difference between sensible and latent heat change for a solid-liquid change. The temperature remains constant during the phase change and extensive amount of heat is stored. It is one of the most important characteristics since PCM materials have different melting points. Once the PCM is completely melted, further supply of heat will only increase in sensible heat. PCM is selected depending on the application and the range of temperature required.
- Liquid-Gas: This phenomenon occurs only when there is huge amount of heat quantity supplied to the system.
- Solid-Solid: It is quite uncommon in nature as only a few materials undergo molecular structure modification to store a large quantity of heat. Its behavior is like solid-liquid transformations, but usually, the latent heat capacity is smaller.

The solid-liquid transformation has comparatively smaller latent heat than solid-gas or liquid-gas. However, these transformations involve only a small change in volume (of the order of 20 % or less). Solid-Liquid transitions have proved [4] to be economically attractive for use in thermal energy storage system. PCMs themselves cannot be used as heat transfer medium. A separate heat transfer medium must be used with a heat exchanger in between to transfer energy from the heat source to the PCM and from PCM to the heat sink. The heat exchanger to be used must be designed specially, in the general view of the low thermal conductivity of PCMs.

Therefore a latent heat energy storage system must consist of the following three components:

- A suitable PCM with its melting point in the desired temperature range.
- A suitable heat exchanger
- A suitable container compatible with the PCM.

2.2 PCM Selection

Wide varieties of PCM are available in the market but it becomes important to select the most suitable one based on the usage. As this research is concentrated on high-temperature we found that Erythritol was the most suitable one for our temperature range. Properties we need to focus while selecting a PCM are [6]:

- Energy density of the material.
- Latent heat of fusion.
- Storage thickness.
- Ratio of latent to sensible heat capacity.
- Ratio of PCM volume to the total volume.
- Critical temperature.
- Thermo-physical properties
 - High thermal conductivity of both phases.
 - Small volume change in phase transition.
 - Repeatable phase change cycle
 - Sharpness of latent heat release and absorption.
 - Large sensible heat per unit volume.
 - Phase change temperature within the the range of application.
- Chemical properties
 - Reversible solidification/melting process.
 - Non-flammable, non-toxic.
 - No chemical degradation with number of cycles.
 - Non-corrosive properties.

2.3 Classification of PCMs

Wide varieties of phase change materials are available based on a range of temperature required. PCMs are generally classified into three types: Organic, Inorganic and Eutectics as shown in Figure 2.

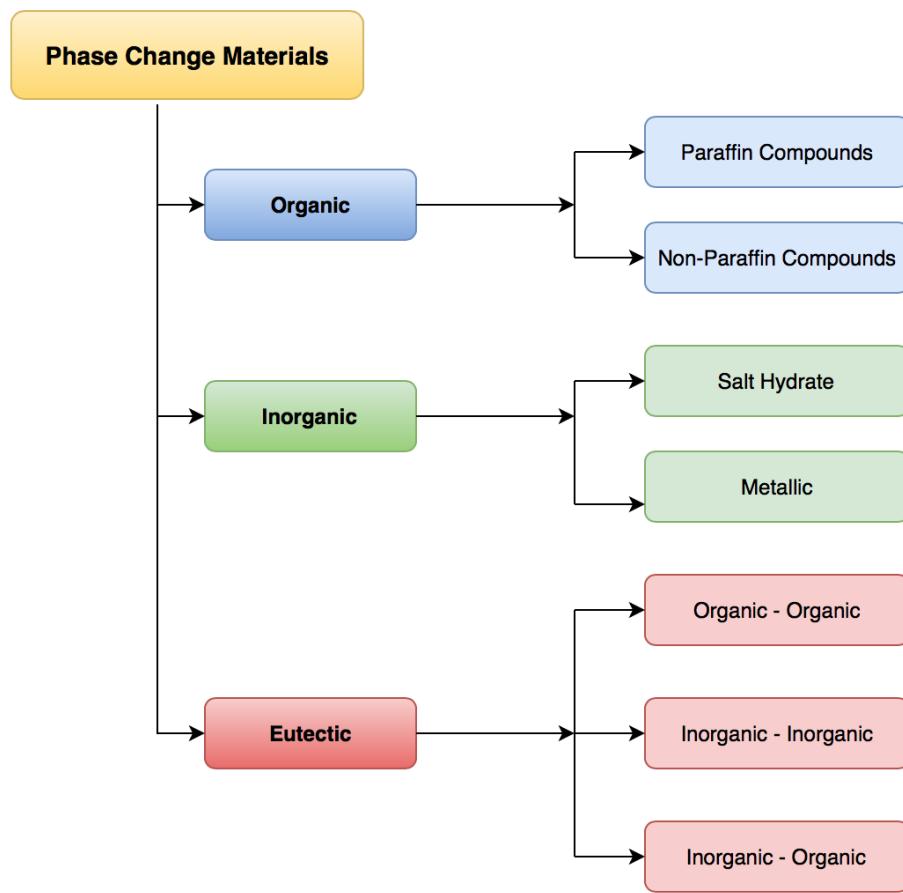


Figure 2: *Classification of Phase change Materials (PCMs)*

2.3.1 Organic PCM

Organic materials are generally categorized into *paraffins* and *non – paraffins*. Usually, this type of materials melts and solidifies congruently, i.e. under repeated melting or solidification cycles, there is no phase segregation. Organic PCMs presents self-nucleation, which is the property of crystallizing with little or no supercooling, and they are not corrosive in nature. Paraffin is further distinguished into paraffin hydrocarbons and paraffin waxes.

2.3.1.1 Paraffin Hydrocarbons

Paraffins hydrocarbons generally consist of straight chains of n-alkanes $CH_3 - (CH_2) - CH_3$, crystallization of this CH_3 chain releases a large amount of latent heat. Melting temperatures of paraffin usually range from 35 to 40 °C and they are most widely used for thermal management of electronic devices. The melting point of these alkanes increases with increase in carbon atoms. Some of the undesirable properties of paraffin are low conductivity, not suitable for plastic container and moderately flammable. Moreover, they have a low density which affects the phase transition at their melting temperature. Common paraffin along with their melting point and heat of fusion are listed in Table 1:

Table 1: *Thermal properties of alkanes.*

n-alkanes at 20°C	Melting Point (°C)	Heat of fusion ($kJ.kg^{-1}$)
Hexadecane	18.1	236
Heptadecane	21.9	214
Octadecane	28.1	244
Nonadecane	32.0	222
Eicosane	36.6	248
Heneicosane	40.2	213
Docosane	44.0	252
Tricosane	47.5	234
Tetracosane	50.6	255
Pentacosane	53.5	238
Hexacosane	56.3	250
Octacosane	61.2	254
triacontane	65.4	252

2.3.1.2 Paraffin wax

Paraffin wax is generally a mixture of alkanes. Since the paraffin hydrocarbons are expensive to obtain it is easier to use paraffin waxes also known as grade paraffin. They possess the same properties as pure alkanes, but their melting point is an average of all the alkanes present in it. Commercial grade paraffin waxes are reported to be able to sustain over 1500 cycles while maintaining their properties unchanged [10]. Unless the practical application defines a precise temperature for the PCM to be melted, paraffin waxes are optimal cost-effective substitutes.

2.3.1.3 Non-paraffin compounds

The non-paraffin compounds are the most numerous of the phase change materials with a wide variety of properties. They are flammable in nature hence they are not applicable for high-temperature storage. Non-paraffin compounds are further distinguished as Fatty acids, Glycols, and Polyalcohols.

- **Fatty acids:** They are normally obtained from animal fats and vegetable oils, they are hydrolyzed obtaining a mixture of different fatty acids that are separated at a later stage. Fatty acids have similar properties to that of paraffin waxes but melt slower, and they are characterized by the general formula $CH_3(CH_2)_{2n}COOH$ [11]. They have desirable properties of PCM such as congruent melting, good stability, biodegradability, and non-toxicity [12]. However, they are mildly corrosive and have high sublimation rate, along with a bad odor [13]. Thermal properties of some fatty acids are listed in Table 2:

Table 2: *Thermal properties of some common fatty acids.* [14]

Common name at 20°C	Melting point (°C)	Heat of fusion ($kJ.kg^{-1}$)
Caprylic acid	16.1	144.2
Capric acid	31.5	155.5
Lauric acid	43.6	184.4
Myristic acid	57.7	189.7
Palmitic acid	61.3	197.9
Stearic acid	66.8	259.0

- Polyalcohols:** These materials and some amines are considered as PCMs since they are characterized by a relatively low enthalpy of fusion. They are also capable of releasing and absorbing a large amount of heat during a solid-solid transition [14-16]. Polyalcohols possess different transition temperatures, hence when they are exposed to a given transition temperature, their structure from low-temperature layer becomes a high-temperature homogeneous face-centered cubic (FCC) crystal structure which has high symmetry and eventually absorbs hydrogen bond energy [17]. Some of the properties are almost null volume change, long lifespan, and no segregation. Properties of polyalcohols are listed in Table 3:

 Table 3: *Thermal properties of solid-solid phase transition for polyalcohols and amine derivatives* [18-19].

Common name at 20°C	Melting point (°C)	Heat of fusion ($kJ.kg^{-1}$)
Pentaerythritol (PE)	187-188	269-289
Pentaglycerine (PG)	81-89	193-269
Neopentylglycol (NPG)	40-48	110-131
Aminoglycol (AMPL)	78	233.6
Tris-aminoCH ₄ (TAM)	134.5	285

2.3.2 Inorganic PCM

Inorganic materials are generally salt hydrates, they are typically an alloy of inorganic salts and water forming a crystalline solid of general formula $A.B.nH_2O$.

2.3.2.1 Salt hydrates

They are the most widely studied PCMs for the latent heat thermal energy storage system, as their melting temperature ranges from 10 to 900 °C. Some of their attractive properties are: high latent heat of fusion per unit volume, relatively high thermal conductivity, small volume change on melting and higher density. Unlike organic materials, the inorganic materials have sharp phase transitions at their melting temperature, which makes it an advantage for the thermal storage system. The major issue with using salt hydrates is that they melt in-congruently (melting occurs when salt is not entirely soluble in its water), hence the solution is supersaturated at its melting temperature [4]. They also have a tendency for supercooling, which

in turn discharges the energy at much lower temperature instead of discharging at fusion temperature. This issue is generally tackled by adding chemicals and stimulating the nucleation to happen. List of some salt hydrates are listed in Table 4:

Table 4: *Thermal properties of some salt hydrates.*

Material at 20 °C	Melting point (°C)	Heat of fusion ($kJ.g^{-1}$)
CaCl ₂ · 12H ₂ O	29.8	174
LiNO ₃ 2H ₂ O	30.0	296
LiNO ₃ 3H ₂ O	30.0	189
KFe(SO ₄) ₂ 12H ₂ O	33.0	173
LiBr ₂ 2H ₂ O	34.0	124
FeCl ₃ H ₂ O	37	223
CoSO ₄ 7H ₂ O	40.7	170
Ca(NO ₃) 4H ₂ O	47.0	153
Fe(NO ₃) ₃ 9H ₂ O	47.0	155
Ca(NO ₃) ₂ 3H ₂ O	51.0	104
FeCl ₃ 2H ₂ O	56.0	90
CH ₃ COONa 3H ₂ O	58.0	265
MgCl ₂ 4H ₂ O	58.0	178
NaAl(SO ₄) ₂ 10H ₂ O	61.0	181
NaOH H ₂ O	64.3	273
Al(NO ₃) ₂ 9H ₂ O	72	155
MgCl ₂ 6H ₂ O	117.0	167

2.3.2.2 Metals

They are basically a combination of low melting point metals and metal eutectics. Although they have some very interesting properties compared with other PCMs, such as high heat of fusion per unit volume, high thermal conductivity, low specific heat and low vapor pressure, they have been little studied because of their very high density [4]. Table 5 reports some compounds that belong to this category.

Table 5: *Thermal properties of metallic compounds .*

Material at 20°C	Melting Point (°C)	Heat of fusion ($kJ.kg^{-1}$)
Gallium	30.0	80.3
Cerrolow eutectic	58.0	90.9
Bi–Cd–In eutectic	61.0	25.0
Cerrobend eutectic	70.0	32.6
Bi–Pb–In eutectic	70.0	29.0
Bi–In eutectic	72	25.0

2.3.3 Eutectics

An eutectic is a material composed of two or more components. They solidify congruently and without segregation at a temperature that is normally lower than the one at which single components solidifies, called "eutectic temperature". Their thermal application is relatively new hence, a limited amount of information is known. They usually have sharp melting points comparable to pure substances and a higher volumetric storage density than organic compounds. Selected eutectics are listed in Table 6:

Table 6: *Thermal properties of Eutectics materials.*

Material at (20°C)	Meting point (°C)	Heat of fusion ($kJ.kg^{-1}$)
Triethylolethane + Water +Urea	13.4	160
$CaCl_2 + MgCl_2 \cdot 6H_2O$	25	95
$CH_3CONHH_2^+ NH_2CONH_2$	27	163
Triethylolethane+urea	29.8	218
$CH_3COONa \cdot 3H_2O + NH_2CONH_2$	30	200.5
$NH_2CONH_2^+ NH_2NO_3$	46	95
$Mg(NO_3)_3 \cdot 6H_2O + NH_4O_3$	52	125.5
$Mg(NO_3)_3 \cdot 6H_2O + MgCl_2 \cdot 6H_2O$	59	132.2
$Mg(NO_3)_3 \cdot 6H_2O + MgBr_2 \cdot 6H_2O$	66	168
$NH_2CONH_2 + NH_4Br$	76	151

2.4 PCM applications

There is a wide variety of applications of phase change materials. They can be used for thermal protection and storage, the difference between these two fields of application relates to the thermal conductivity of the substance. In some cases of thermal protection, it is appropriate to have low conductivity value, while in a storage system such low value can produce a real problem since there can be sufficient energy stored but an insufficient capacity to dispose of this energy quickly enough. In general PCMs application can be broadly classified in low-temperature and high-temperature applications.

2.4.1 Low temperature

Regarding low-temperature applications the melting temperature of the PCMs is generally below 20 °C. Application of such PCMs is reported in the protection of solid food and beverages, pharmaceutical products, electronic circuits, spacecraft, air conditioning and industrial refrigeration. Water is one of the most used substances for low-temperature application due to its properties like low cost, high thermal conductivity, long stability and no toxicity [6].

2.4.1.1 PCM in spacecraft applications

The application of PCMs has not been limited to passive thermal control for ground equipment alone. The recent research and development in PCMs can be extended

for spacecraft systems [35]. In the area of heat removal and dissipation, the applicable technologies for spacecraft are high thermal conductivity materials, high heat transport devices such as fixed conductance heat pipes, loop heat pipes etc. The simplest form of PCMs thermal control for electronic components is the one that is used for short-duty cycle components in launch or reentry vehicles. During this process, there is a large amount of heat generated which has to be extracted to avoid over-heating and subsequent failure of the electronic components. This generated heat is absorbed via latent heat of fusion by the PCMs without an appreciable temperature rise of the components.

Some of the application of PCMs in spacecraft technologies are [35]:

- Onboard power generation using thermal energy.
- Electronic components having cyclic operating conditions.
- Enhance efficiency of fluid-loop/radiator systems.
- Universal Spacecraft Thermal Control Architecture.
- Precise dimensional stability.
- Micro/nano satellites.

2.4.1.2 PCMs in building

PCMs have been considered for thermal storage in buildings for a long time. With the advent of PCMs implemented in wall-boards, shutters, under-floor heating systems and ceiling boards, they can be used as a part of the building for heating and cooling applications. Another interesting possibility in building applications is the impregnation of PCMs into porous construction materials, such as plasterboard, to increase the thermal mass [39]. The application of PCMs in buildings can have two different goals. First, using natural heat that is solar energy for heating or cooling. Second, by using a heat source or sink. Storage of heat is necessary to match the availability and demand with respect to time and with respect to power generated. There are two ways to use PCMs for building applications:

- PCMs in building walls.
- PCMs in heat and cold storage units, e.g. air-conditioner.

PCMs can be used to store cold for air conditioning applications, where cold is collected and stored from ambient air during the night, and it is released to the indoor ambient during the hottest hours of the day. This concept is known as free-cooling [40].

2.4.2 High temperature

PCM having melting temperature above 80 °C can be used for high temperature storage units. Our study falls under the classification of high temperature as the melting temperature of erythritol PCM is around 118 °C. In our case PCM is wrapped around the stove pipe of wood stove to store heat energy and release it when it is needed. One more option of using PCM in wood stove is to attach this PCM on the walls of wood stove to store heat.

Fabio et al.[41] studied thermal analysis of a novel thermal energy storage based on high-temperature phase change material to improve efficiency in waste-to-energy plants. The study was carried out by replacing the typical refractory brick installed in the combustion chamber with a PCM-based refractory brick capable of storing a variable heat flux and to release it on demand as a steady heat flux. It showed that there was an increase in efficiency up to 34 % from the conventional waste energy plant.

3 Heat transfer in phase change materials

As a material undergoes melting or solidification there is phase transformation, which is a discontinuous change of the properties of the substance. When phase transition occurs, latent heat is either absorbed or released by the thermodynamic system without changing the temperature. The heat transfer mechanisms associated with the melting and solidification process is generally either conduction or convection (natural convection) or simultaneous conduction/convection. Such problem was first solved by Stefan and is normally called a classical Stefan problem. This classical Stefan problem aims to describe the temperature distribution in a homogeneous medium undergoing a phase change, this is accomplished by solving the energy equation with Stefan boundary condition. The energy equation at the solid-liquid interface phase is given as [4]:

$$\lambda\rho\left(\frac{ds(t)}{\delta t}\right) = k_s\left(\frac{\delta T_s}{\delta t}\right) - k_l\left(\frac{\delta T_l}{\delta t}\right) \quad (3)$$

where λ is the latent heat of fusion of the PCM, T_s and T_l are the solid and liquid phase temperatures, k_s and k_l are the thermal conductivities of the solid and liquid PCM, s is the phase front of the PCM and ρ is the density of the PCM.

3.1 Latent heat TES design challenges

Most classes of pure PCMs exhibit a low thermal conductivity, although the inorganic PCMs have relatively higher conductivity when compared to organic ones [20]. Consequently, the low thermal conductivity leads to poor heat exchange between the PCMs and the heat transfer fluid (HTF) and hence, the need for enhancement. The most common enhancement techniques involve the use of extended surfaces such as fins, heat pipes and multiple PCMs for a different melting point. Nanocomposite

carbon nanofibre (CNF) can be also used to improve the thermal conductivity of PCMs [21]. Some techniques of enhancement are shown in Figure 3.

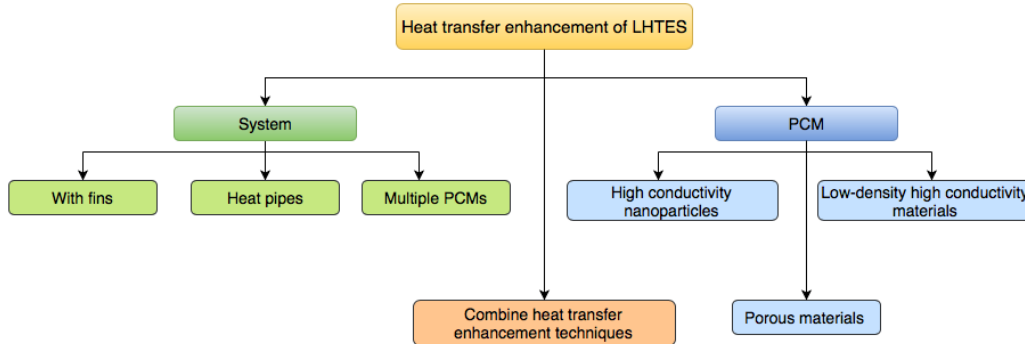


Figure 3: *Techniques for heat transfer enhancement of LHTES system.*

3.2 Heat transfer enhancement

Improving the heat transfer in PCMs is another important option for enhancing the overall thermal performance of LHTES system. In general thermal conductivity of PCMs can be improved by addition of fins, porous materials of high thermal conductivity, dispersion of high conductivity materials/nanoparticles.

Fins are generally used to increase the heat transfer area between PCMs and HTF and consequently improve the thermal performance of LHTES system. Selection of the fin material depends on its thermal conductivity, density cost, and corrosion potential. Some of the widely used fins materials are listed in Table 7. Graphite foil appears to have the advantage of low density, while aluminum has the advantage of relatively high thermal conductivity, low cost and medium density as compared with other materials.

Table 7: *Properties of common fin materials.*

Material	Thermal conductivity ($W/m - K$)	Density (Kg/m^3)
Graphite foil	150	1000
Aluminum	200	2700
Stainless Steel	20	7800
Carbon steel	30	7800
Copper	350	8800

The most widely used fins configuration is radial and vertical fins. Agyenim et al. [37] considered two concentric tubes storage units with radial and vertical fins as shown in Figure 4. The authors compared the thermal performance of the two configurations experimentally and the results showed that the system with vertical fins provided the best thermal response during melting.

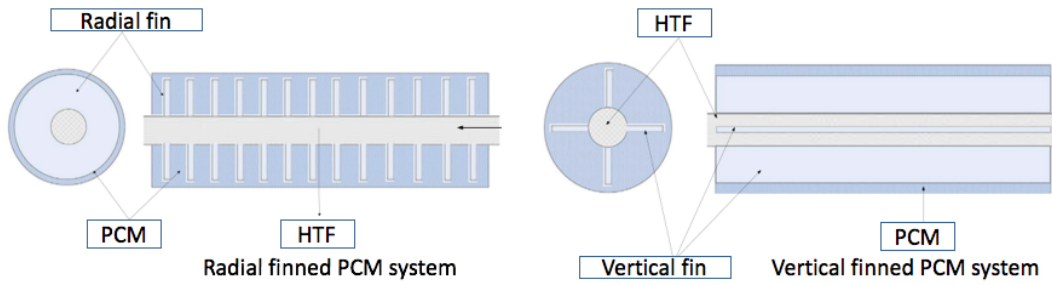


Figure 4: *General types of fins*

3.3 Application of heat pipes

The heat pipe (HP) behaves as a thermal carrier between the HTF and PCM by evaporation and condensation process of its working fluid occurring in the evaporator and condenser respectively. The use of HP in LHTES system is a promising and important technique for accelerating the melting and solidification processes of PCM especially in systems involving cyclic melting and solidification. Heat pipes can be made in different shapes, sizes and operate in specific temperature range passively. The choice of the type of HP and its working fluid for thermal energy storage enhancement depends on the operating temperature, size and geometrical configuration of the storage system.

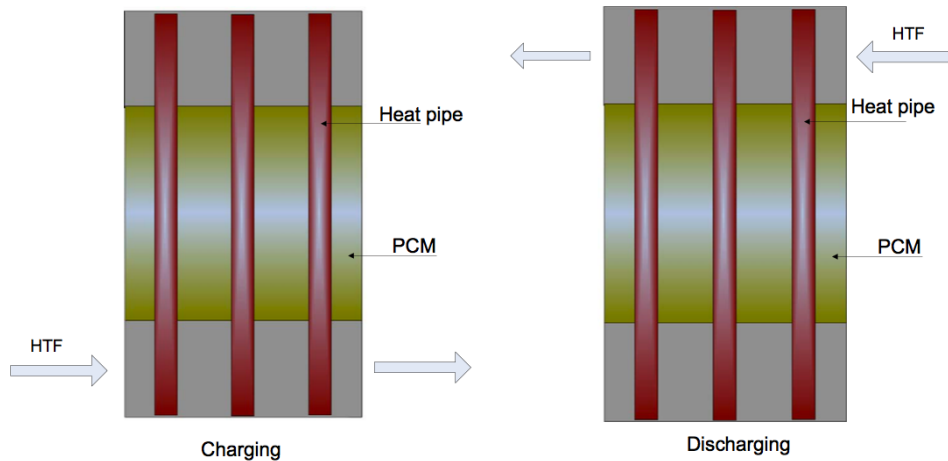


Figure 5: *Cascaded configuration of LHTES system during charging and discharging.*[36]

Heat pipes can be embedded in cascade latent heat storage system where one or more channels of HP can be used for charging and discharging of the system [36]. Figure 5 shows HPs inserted perpendicular to the HTF flow direction passing across the PCM, thereby increasing the heat transfer rate between the HTF and the PCM.

3.4 Multiple PCMs

The use of multiple PCMs in LHTES system is another technique for heat transfer enhancement. The purpose of multiple PCMs is to maintain a nearly constant temperature difference between the HTF and the PCMs during charging and discharging cycles, thereby increasing the thermal performance of the LHTES system. In a typical shell-and-tube LHTES system, multiple PCMs of different melting temperatures are arranged in a decreasing order of their melting points along the flow direction of HTF during the charging process, as shown in the Figure 6. This trend leads to nearly a constant heat flux to the PCM. The HTF flow direction is reversed during the discharging the cycle and hence, the PCMs remain in the increasing order of their melting points and nearly a constant heat flux from the PCM to HTF can be obtained [25].

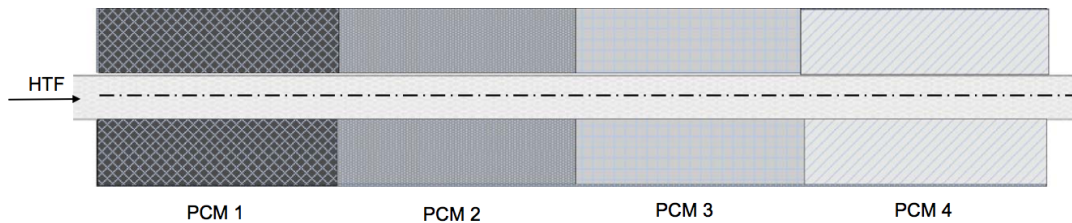


Figure 6: *Schematic of multiple PCMs in shell-and tube LHTES unit*

Effects of different multiple PCMs on the performance of a LHTES unit have been studied numerically by Fang and Chen [26]. They reported that the difference in melting temperature between the multiple PCMs is crucial for performance enhancement of LHTES and hence, should be taken into account. Gong and Mujumdar [27] developed a novel storage unit with multiple PCMs. The unit consists of a tube into which HTF flow and an outer coaxial cylinder containing several segments of different PCMs. They investigated the heat transfer characteristic of the unit during the melting and the freezing processes using finite element approach. Their results revealed that using composite PCMs can significantly reduce the fluctuation of the outlet temperature of the HTF and about 33.8 % enhancement in energy charge-discharge rate was achieved as compared with a single PCM.

3.5 Effect of porous materials

Impregnation of porous materials is the fastest growing method for enhancing the thermal conductivity of the conventional PCMs in LHTES system. This is primarily due to higher magnitude of thermal conductivity of the porous material than the pure PCMs [28]. Siahpush et al. [29] studied the thermal performance of a solid/liquid phase change of LHTES system consisting of eicosane as the PCM and copper porous foam of 95 % porosity. They showed that the presence of copper foam increased the effective thermal conductivity from 0.423 W/mK to 3.06 W/mK. This eventually resulted in the decrease of freezing time of the PCM from 375 min to 85 min, and the melting time from 500 min to 250 min.

Aluminium foam and expanded graphite (or graphite foam) are the most widely used as thermal conductivity enhancers. This is due to their relatively low or medium density and high thermal conductivities.

3.6 Dispersion of nanoparticles

Significant progress on the use of high conductivity nano-materials combined with PCMs to enhanced their thermal conductivity has been achieved recently. This includes the use of nanopowders (such as Al, CuO, Cu, SiC), nanowires (NW) and carbon nanotubes (CNT). Mettawee et al. [30] investigated the effect of aluminum powder on thermal conductivity enhancement of paraffin wax contained in a compact PCM solar collector. The experimental results showed about 60 % reduction of the charging time by adding the aluminum powder in the wax. The useful heat gained was increased when the aluminum powder was added in the wax during the discharging process as compared with the case of pure paraffin wax.

Cui et al.[31] studied the thermal properties of carbon nanofibre (CNF) and carbon nanotube (CNT) filled PCMs (soy wax and paraffin wax). They formed the composite PCMs by stirring of CNF or CNT in a liquid wax at 60 °C, with CNF and CNT doping levels of 1, 2, 5, and 10 wt%. The results indicate that both CNF and CNT can improve the thermal conductivity of the composite, with CNF being more effective than CNT due to its better dispersion in the matrix.

3.7 Dispersion of low density materials

Metal particles/structures have relatively high densities which usually leads to their settlement at the bottom surface of the PCM container, making the storage system gain a considerable weight. Hence, many researchers consider other alternatives such as low-density high-conductivity additives for PCM.

Carbon fibers can be better alternatives to enhance the thermal performance of the LHTES system since they have relatively lower densities than metals and their thermal conductivity is almost equivalent to aluminum and copper. Carbon fibers also exhibit high corrosive resistance potential and hence are compatible with most of the PCMs. Carbon fibers with a high thermal conductivity embedded into paraffin PCMs can enhance the overall thermal conductivities in heat storage system as confirmed by Fukai et al. [32]. They used randomly oriented fibers and fiber brush as shown in Figure 7. The results indicate that the carbon fibers enhanced the effective thermal conductivity of paraffin composites. The fiber length showed little effect on the effective thermal conductivity while the fiber brush increased the effective thermal conductivities to the maximum theoretical values. Fukai et al. [33] reported that the transient thermal responses in carbon fiber/n-octadecane composites PCM significantly improved as the volume fraction and the diameter of the fibers increased. However, any further improvement above a critical diameter is not expected due to thermal resistance between the fibers and the tube surface. Fukai et al. [34] reported that carbon brushes significantly improved the rate of

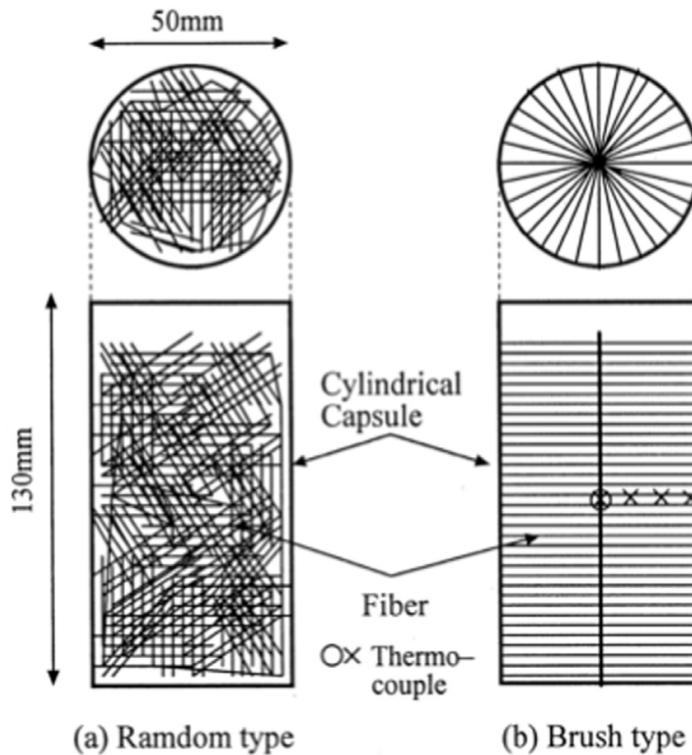


Figure 7: Arrangements of carbon fibers in cylindrical capsules [32]

heat exchange during the charging and discharging processes even at low volume fractions of the fibers.

4 Mathematical and numerical modeling of LHTES system

Phase change processes exhibit a transient and non-linear phenomenon with a moving liquid-solid interface and involve flow problems associated with HTF. Consequently, predicting the behavior of phase change processes is challenging. Two numerical methods are widely used to model the phase change: effective heat capacity method or enthalpy formulation method [22]. In addition to these approaches, the temperature-transforming model is also used to simulate the phase change process [23].

4.1 Moving boundary problems

The heat transfer problem in melting and solidification processes is called moving boundary problems. It is especially complicated due to the fact that the solid-liquid boundary moves depending on the speed at which the latent heat is absorbed or lost at the boundary. While in theory phase change occurs at one defined temperature, in practice it happens over a temperature range, forming a so-called mushy zone (two-phase zone) between liquid and solid. Hence, it becomes more relevant to solve

the problem by enthalpy formulation method. Enthalpy method treats the enthalpy as a temperature-dependent variable and builds the latent heat flow through the volume integration with the use of enthalpy of the system.

4.2 Effective heat capacity method

For the effective heat capacity method, the latent heat capacity of the PCM during phase change process is approximated over a phase change temperature interval. The effective heat capacity is directly proportional to the energy gained/released during the phase change process but inversely proportional to the melting or solidification temperature range. Latent heat stored during the phase change can be evaluated using effective heat capacity-temperature dependence:

$$H = \int_{T_s}^{T_l} c_{eff} dT \quad (4)$$

The governing energy equation for PCM can be expressed as:

$$\rho c_{eff}(T) \frac{\partial T}{\partial t} = \nabla(k \nabla T) \quad (5)$$

where:

$$c_{eff} = \begin{cases} c_p, & \text{if } T_s < T < T_l \\ \frac{L}{T_s - T_l} + c_p(T_l), & \text{if } T_l \leq T \leq T_s \end{cases}$$

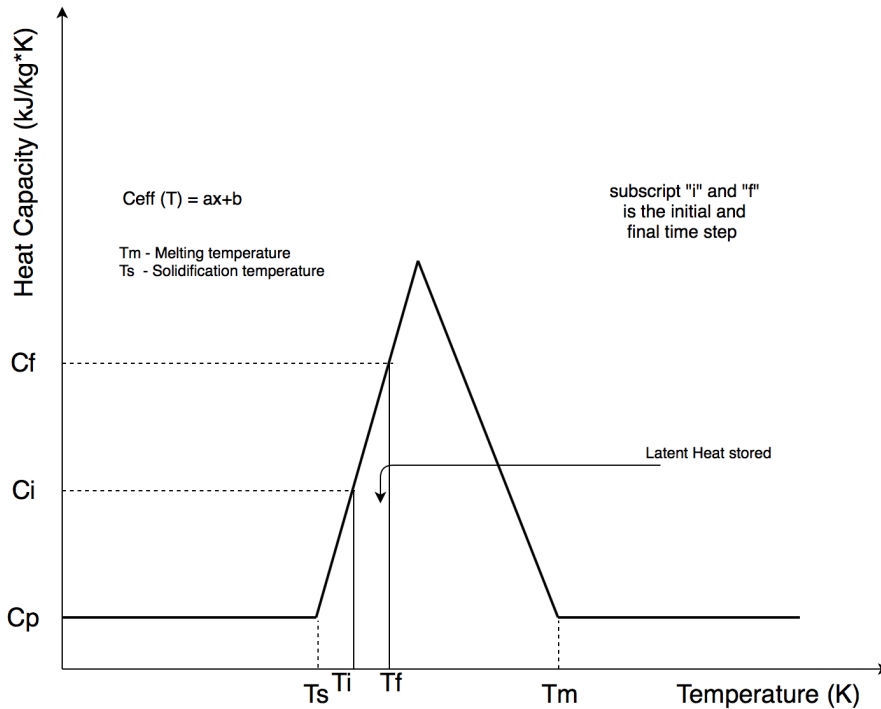


Figure 8: Graphical representation of effective heat capacity method.

where L is the latent heat, T_s and T_l are the solid and liquid temperature of the PCM and c_{eff} is the effective heat capacity.

Available methods for solving the mathematical models include finite difference, finite element, and finite volume approaches. The finite volume approach is the most relevant for the present case study since the CFD simulation is performed with FLUENT 17.2. A high number of numerical studies have been conducted to examine the heat transfer and thermal performance of enhanced LHTES systems. They were mainly concerned with the evaluation of melting/solidification rates, heat transfer rate, and amount of heat stored/released as compared to the system without enhancement.

4.3 Enthalpy formulation method

Using the enthalpy formulation method, the enthalpy is considered as a temperature dependent variable and the flow of the latent heat is expressed in terms of volumetric enthalpy as a function of a temperature of the PCM. The enthalpy formulation is one of the most popular fixed-domain methods for solving Stefan problem. The major advantage is that the method does not require explicit treatment of the moving boundary. To introduce the formulation, we define an enthalpy function "h" as a function of temperature and equations are applied over the fixed domain as given by Voller [8]. This method assumes that enthalpy is a sum of sensible and latent heat [8]:

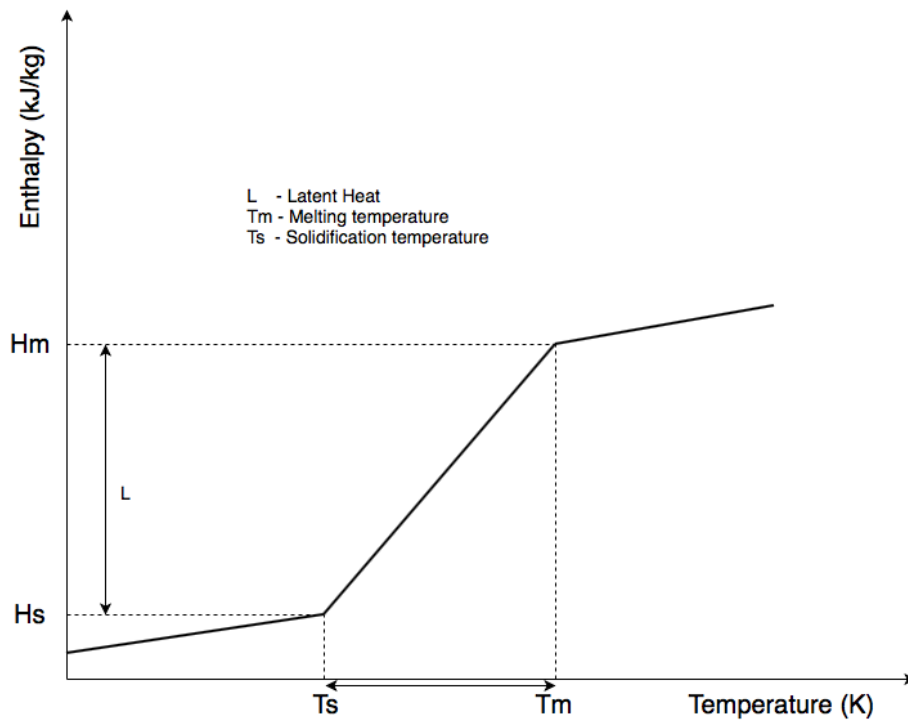


Figure 9: Graphical representation of the enthalpy formulation method.

$$H(T) = h(T) + L\beta(T) \quad (6)$$

where:

$$h(T) = \int_{T_s}^{T_l} c_p dT \quad (7)$$

and liquid fraction β is given as:

$$\beta = \begin{cases} 0, & \text{if } T \leq T_s \\ 1, & \text{if } T \geq T_l \\ \frac{T-T_s}{T_l-T_s}, & \text{if } T_l \leq T \leq T_s \end{cases}$$

One interesting feature of the enthalpy method is that the conduction equation is valid for both the solid and liquid phases as well as for the solid-liquid interface and hence, there is no need to track the position of phase change front [24]

The main advantages of this procedure are:

- The equation is directly applicable for 3 phases (solid, liquid and mushy zone).
- The temperature is determined at each point and the thermophysical properties can be evaluated.
- With the temperature field it is possible to spot the position of the two boundaries.

4.4 Governing equations used in ANSYS Fluent

Modelling of the LHTEs system has been performed using ANSYS Fluent 17.2 and is based on enthalpy-porosity formulation. In this technique, the melt interface is not tracked explicitly[9]. Instead the liquid fraction, which indicates the fraction of the cell volume that is in a liquid form associated with each cell domain is tracked. This liquid fraction is computed at each iteration, based on the enthalpy balance. In the mushy zone, liquid fraction lies between 0 to 1 and it generally decreases from 1 to 0 as the material solidifies. The continuity, momentum, and energy equations are given below:

Continuity equation:

$$\frac{\partial u}{\partial x} + \frac{\partial v}{\partial y} = 0 \quad (8)$$

Momentum equation:

$$\frac{\partial(\rho V)}{\partial t} + \nabla \cdot (\rho V) = -\nabla P + \mu \nabla^2 V + \rho g + S_i \quad (9)$$

The source term in the momentum equation is define as:

$$S_i = \frac{(1 - \beta)^2}{(\beta^3 + \varepsilon)} C V \quad (10)$$

where V is the fluid velocity vector, ρ is the density, μ is the dynamic viscosity, P is the pressure, g is the gravitational acceleration, S_i is the momentum source term, C is a constant term to reflect mushy zone morphology and k is the thermal conductivity.

The enthalpy-porosity technique treats the mushy region as a porous medium. The porosity in each cell is set equal to the liquid fraction in the cell. S_i is the porosity function introduced by Bernt et al. [10], which follows from the Carman Kozeny equations for the flow across the porous media. Here, C determines the rate of velocity reduction to zero when the material changes from liquid to solid. The value is varied from 10^4 to 10^7 according to the PCM property and ε is a small number (0.001) used to prevent division by zero [1].

Energy equation:

$$\frac{\partial}{\partial t}(\rho H) + \nabla \cdot (\rho V H) = \nabla \cdot (k \nabla T) \quad (11)$$

Where ρ is the density of the PCM, V is the fluid velocity, g is the gravity accelerated, k is the thermal conductivity, H is the specific enthalpy and h is the sensible enthalpy and it can be express as:

$$h = h_{ref} + \int_{T_{ref}}^T c_p dT \quad (12)$$

The enthalpy H can be expressed as:

$$H = h + \Delta H \quad (13)$$

Where h_{ref} is the reference enthalpy at the reference temperature T_{ref} , c_p is the specific heat capacity, ΔH is the latent heat content that may change between zero (solid) and L (liquid), the latent heat of the PCM, and β is the liquid fraction during the phase change between the solid and liquid state when the temperature is $T_l > T > T_s$ and it can be written as:

$$\beta = \frac{\Delta H}{L} \quad (14)$$

$$\beta = \begin{cases} 0, & \text{if } T \leq T_s \\ 1, & \text{if } T \geq T_l \\ \frac{T-T_s}{T_l-T_s}, & \text{if } T_l > T > T_s \end{cases}$$

4.5 Effect of mushy zone constant

C is an important parameter for accurately modeling phase change phenomenon; with higher C values corresponding to a delayed melting of the PCMs. The C represents the magnitude of the damping term used in the momentum conservation equation. Higher C values result in the fluid with the mushy region approaching a static state more quickly, which in turn reduces the convective heat transfer across the region [7].

According to literature C value is usually varied from 10^4 to 10^7 . So, to better understand the C value and to find the most appropriate value for our case, 2D simulation for a range of values were performed with a simple geometry dimension of 0.05×0.05 m. A constant temperature of 498 K is applied to the inner-wall pipe and a comparison on the effect of the melt fraction is shown in Figures 10 & 11. From the results, it is clearly seen that with a C value of 10^4 , the solution is unstable and the melting rate is comparatively faster than other cases. For the C values 10^6 and 10^7 , it is seen that the melting rate is relatively low as it dampens the effect of natural convection occurring in the melted PCM hence it behaves like the mode of heat transfer is only due to conduction. However, for a C value of 10^5 , the solution is stable and it takes into account of both conduction and convection as the mode of heat transfer. It also shows a good agreement with the literature [1-5]. Hence, a C value of 10^5 was selected for rest of the simulation cases in this research study. It was also noticed that C values have a huge effect on the temperature difference ΔT between the solid and liquid temperature of the PCM. It was observed that ΔT value of 3 (K) gave the best stable solution for our case, as with lower ΔT there was sharp gradient during phase change process.

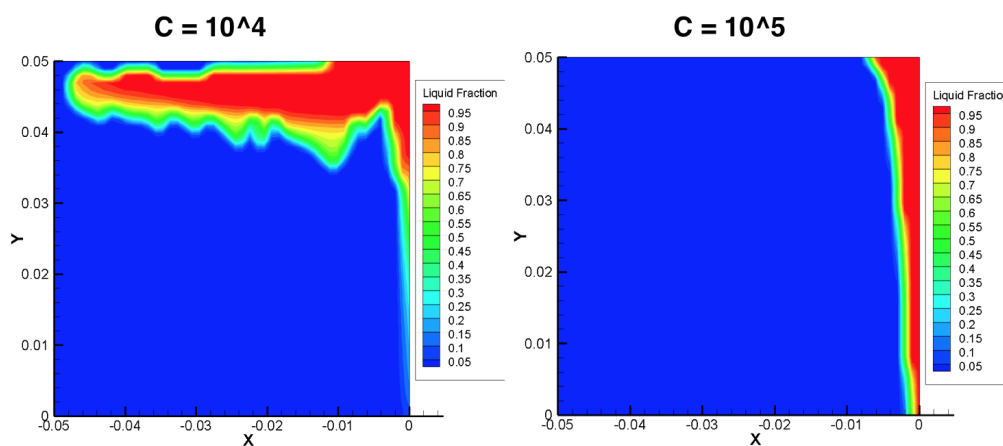


Figure 10: *Effect of C values (10^4 and 10^5) on melting process after 10 min.*

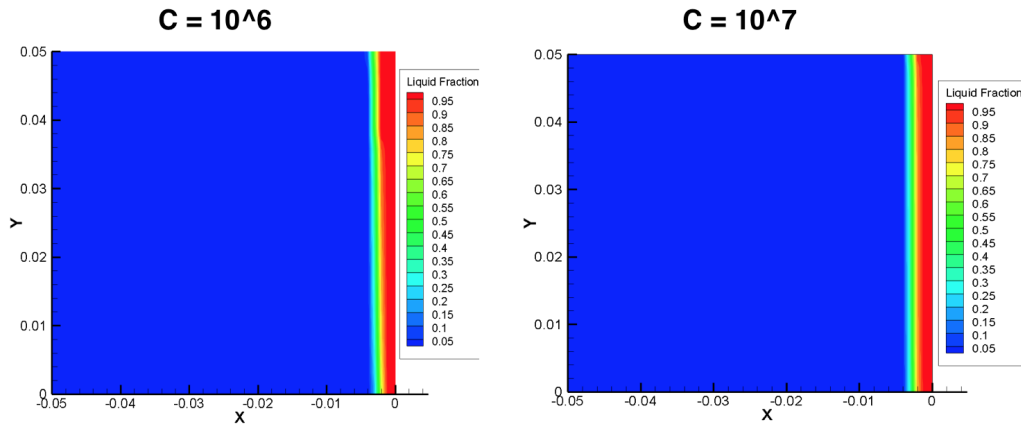


Figure 11: *Effect of C values (10^6 and 10^7) on melting process after 10 min.*

4.6 Numerical solution with conduction and convection

Conduction-controlled phase change is the phase change in which conduction is assumed as the major mechanism of heat transfer through the PCM. For convection-controlled phase change, the assumption is that the PCM melting process is mostly affected by convection. In the case of conduction/convection phase change, both conduction and convection are considered to play major roles during the transition stages.

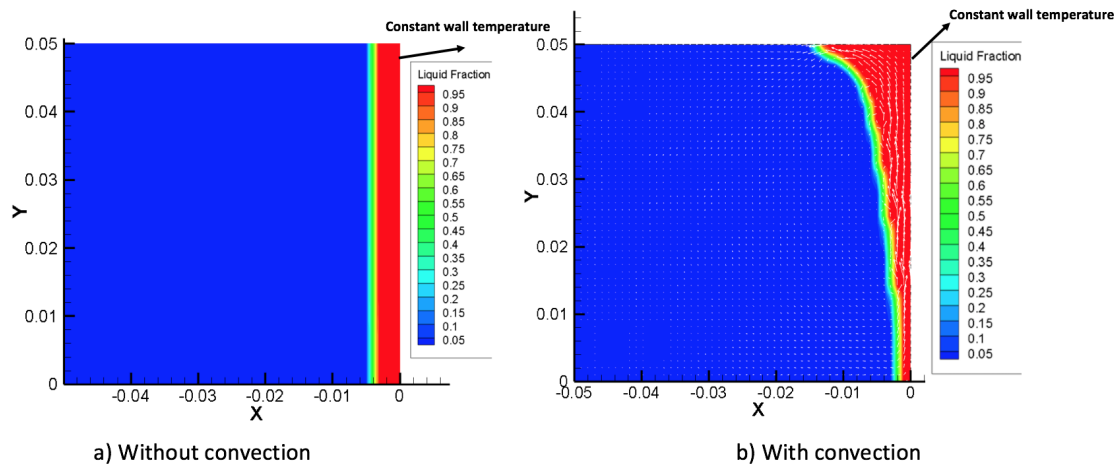


Figure 12: *Effect of convection on PCM melting process after 15 min.*

Initially, the effect of convection was neglected to simplify the simulation i.e. assuming that the gravity term in momentum equation is zero. This implies that heat transfer to the PCM from the hot wall is only due to conduction. In Figure 12a it can be seen that the rate of melting is uniform across the PCM section when the mode of transfer is just conduction. In order to make the system closer to

reality, the gravity term is introduced ($-9.81 \text{ m}^2/\text{s}$) in the y-direction. In doing so, it was noticed that the melting in PCM was no more uniform Figure 12b, due to the temperature-dependent density of the PCM and the buoyancy effect. The induced natural convection increases the rate of heat transport towards the top of the PCM storage and increased the overall melting rate.

5 Modeling methods

5.1 Geometry specification

In the present case of a stove pipe, cylindrical geometries are considered the most promising configuration for a heat exchanger, such as a double pipe heat exchanger. As shown in Figure 13, the stove pipe of the wood stove is used as heat storage unit. PCM is wrapped around the stove pipe to extract heat, store it and eventually supply the heat to the surrounding.

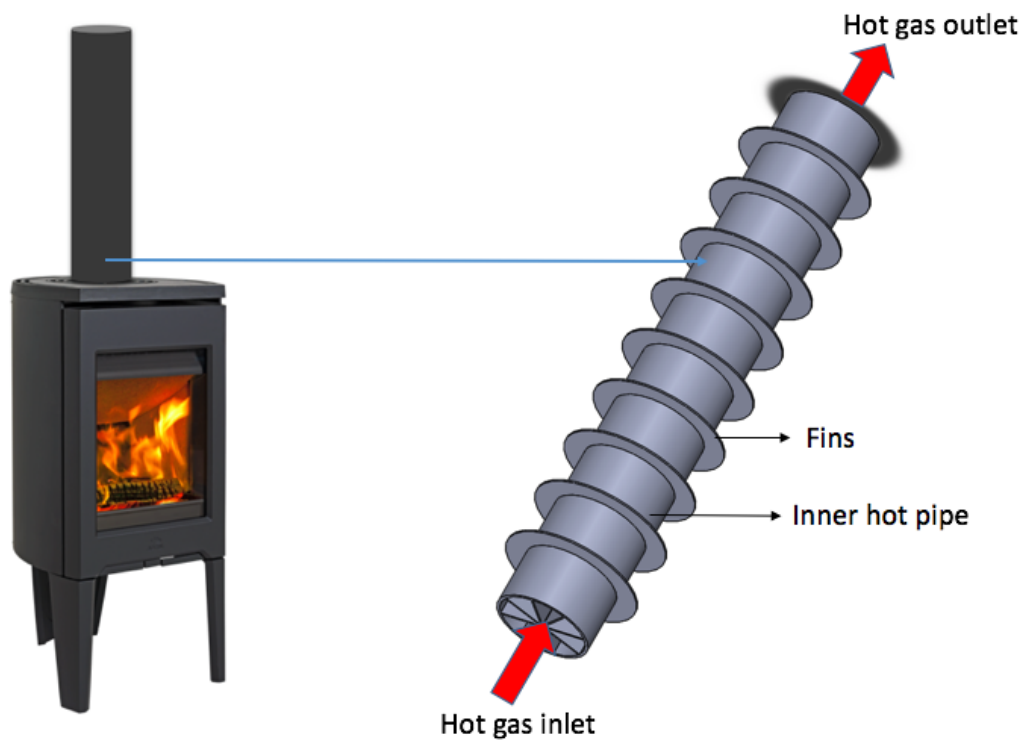


Figure 13: *wood stove pipe and fins*

The geometry includes vertical fins in the hot gas flow side and radial fins on the PCM side. The dimensions of the model are listed below:

- Length: 1 m
- Outer diameter of inner pipe: 0.15 m
- Outer diameter of outer pipe: 0.3 m
- Radial fins: 0.035 m
- Vertical fins: 0.065 m
- Thickness of fins: 0.003 m
- Thickness of PCM : 0.07 m

To simplify the geometry and to reduce the computational cost, the dimension of the length of the pipe was reduced to 300 mm and was considered as a 2D axisymmetric model by keeping the rest of the dimension same.

5.1.1 Fins in hot gas domain

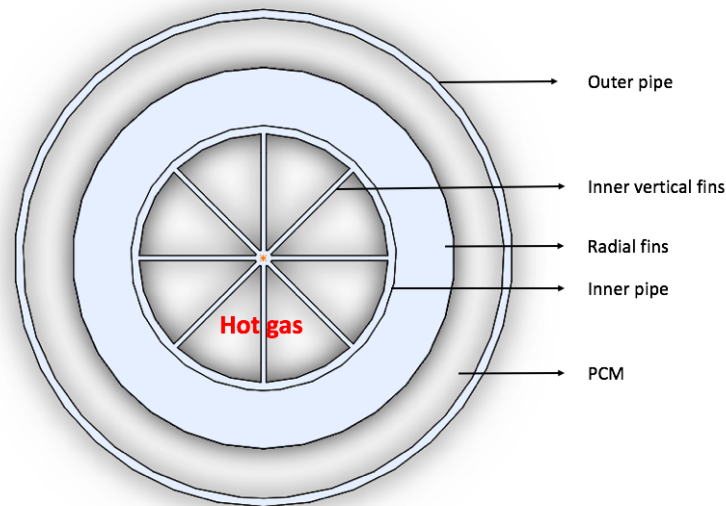


Figure 14: *Top view of the wood stove pipe*

Initially, the geometry was considered without the presence of fins in the hot gas section, but it was noticed that insufficient heat was supplied to the PCM to melt it. This is due to the poor conductivity of hot gas and temperature. Since it was necessary to melt the PCM to store the heat in the form of latent heat another design was taken into account as it is not possible to change the properties of a hot gas. There were two design to increase the heat transfer from the hot fluid to the pipe: 1. fins and 2. honeycomb structure attached to the pipe. But, having a honeycomb structure inside the pipe will increase the collection of soot particles and increase the maintenance or fire risk, hence vertical fins were selected instead of honeycomb structure. Specifically 8 fins were chosen to have a more uniform heat distribution to the inner pipe. Once, this was installed it was noticed that the effective thermal conductivity was increased to 2.45 (W/(m.K)) instead of 0.035 (W/(m.K)) , which ultimately resulted in must more heat transfer to the PCM domain. However, it was not physical for us to represent the presence of vertical fins in 2d axisymmetric geometry hence effective thermal conductivity of air was taken as 2.45 (W/(m.K)) . The calculation table of improved thermal conductivity is shown in Figure 15 :

5.1.2 Mesh specification

While solving a numerical solution the quality of mesh plays a vital role as it directly affects the accuracy and stability of the numerical computation. Hence, a closer look was made to have a sufficient mesh quality. First, it was made sure that the aspect ratio of the whole geometry mesh is in the range between 18 to 45. It is also

16. The full report of the mesh quality of this geometry is included in the Appendix.

Another important aspect is to create mesh interfaces between the walls, hot gas fluid, PCM, and fins. If this interface is not taken into account then there would not be proper heat transfer from one domain to another.

5.2 Types of model

Our study was carried out for two different models of LHTES system:

- Constant wall temperature 415 (K) in the inpipe.
- Hot gas flowing in the stovepipe with an inlet temperature of 498 (K).

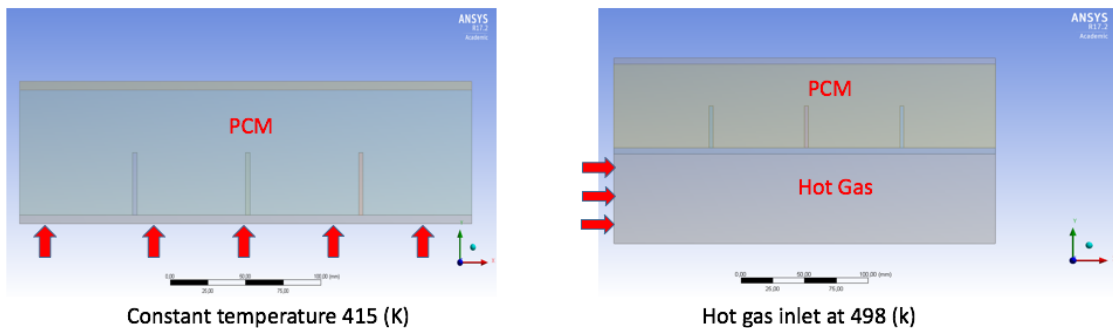


Figure 17: *2D axisymmetric constant wall temperature and hot gas inlet temperature models*

Table 8: *Fin length in LHTES system.*

Cases	Fin length (mm)	Fin thickness (mm)
Case A	-	-
Case B	17,5	3
Case C	35	3
Case D	52,5	3
Case E	70	3

Table 9: *Fin frequency in LHTES system.*

Cases	Fin length (mm)	No. of fins
Case F	-	-
Case G	35	1
Case H	35	2
Case I	35	3

The physical configuration of a 2D axisymmetric heat exchanger is shown in Fig-

ure 17, the thickness of the PCM block is 70 mm, the thickness of hot gas domain is 75 mm, an inner pipe and outer pipe thickness are 5 mm and thickness of fins is 3 mm.

All the pipes and fins are considered to be made of stainless steel to ensure good thermal conductivity and to enhance heat transfer between the heat transfer fluid (HTF) and the PCM. Different fin lengths and frequencies were implemented to the inner pipe to understand the effects of fins on melting and solidification of PCM. A list of cases is shown in Tables 8 & 9. After numerous studies, it was noted that having 3 fins for 300mm long pipe was the best case, hence the study of the effect of the fin lengths was carried out for 3 frequency fins.

5.3 Computational methodology

The geometry was created in ANSYS-workbench DesignModeler as well as the mesh of the geometry. The mesh was imported to ANSYS FLUENT 17.2, the simulation was run with the two-dimensional double precision (2 ddp) code. For FLUENT to be able to recognize the two different fluid materials used in HTF and the PCM domains, following setting as shown in Table 10 were used to run the simulation. Further, in cell zone conditions, fins, inner-pipe and outer-pipe were assigned to solid (steel), PCM and hot gas to fluid erythritol and hot gas respectively.

Table 10: *Setup for FLUENT simulation.*

Description	Type
Solver	Pressure-Based
Velocity Formulation	Absolute
Time	Transient
Gravity	On
Energy	On
Viscous	Laminar* / k-epsilon model*
Solidification & Melting	On

*Depending on type of geometry model.

Gravity was set to -9.81 m/s^2 along the y-axis to include the natural convection in the PCM during the simulation process. Hot gas is used as the HTF, erythritol with phase change capability is used as the PCM, properties of erythritol assign in FLUENT are listed in Table 11. It was assumed that hot gas has the following composition: 7 % CO_2 , 13 % O_2 , 20 % H_2O and 60 % N_2 . After inputting this composition in Gaseq the following properties of hot gas are found: density 0.72 kg/m^3 , conductivity 0.024 W/(m.K) , dynamic viscosity of $2.46 * 10^{-5} \text{ kg/ms}$ and specific heat of 1155 J/kg - K .

Table 11: *Thermophysical properties of erythritol PCM.*

Physical properties	Values
Melting temperature	118 ($^{\circ}\text{C}$)
Degradation temperature	160 ($^{\circ}\text{C}$)
Melting heat	339.9 (kJ/kg)
Specific heat Capacity (fluid, 140°C)	2.76 (kJ/kgK)
Specific heat Capacity (solid, 20°C)	1.38 (kJ/kgK)
Conductivity (fluid)	0.326 (W/mK)
Conductivity (solid 20°C)	0.733 (W/mK)
Density (fluid 140°C)	1300 (kg/m^3)
Density (solid 20°C)	1480 (kg/m^3)

5.3.1 Initial and boundary conditions

In the present case, two sets of initial and boundary conditions were used as we carried out simulations for two different axisymmetric models i.e constant wall temperature inlet and with an inlet velocity of hot gas temperature with 498 K.

- Constant wall temperature:** For the melting case the inner-pipe was set to have constant temperature of 415 K. The outer-pipe with the room is set to have mixed thermal conditions i.e. heat is transferred from the outer-wall due to convection and radiation, heat transfer coefficient for convection is set to 25 ($\text{W}/\text{m}^2\text{K}$) with a free-stream temperature of 298K. Similarly, for the radiation, the wall emissivity is set to 0.85 and free-stream temperature to 298 K. The whole LHTES system is at 298 K as initial condition.

In the solidification case it was considered that PCM is completely melted, this is made possible by patching the temperature of PCM above its melting temperature (391 K). We patch the temperature of the inner and outer pipe, and the value of the temperature is based on the temperature reached during the melting case. In this case, we assume that there is heat lost from both inner and outer pipe due to convection and radiation. The boundary condition of the outer pipe remains same as that of the melting case, but the inner pipe is considered to have following boundary conditions: heat transfer coefficient of 25 ($\text{W}/\text{m}^2\text{K}$) and emissivity of 0.7 with free stream temperature of 373K.

- With hot gas velocity inlet at 498 K:** In melting case the inlet boundary was set to velocity-inlet with a value of 1 (m/s), with a constant temperature of 498 K. The outlet boundary was set as outlet-vent. In mesh interfaces zone it was made sure that hot-gas is coupled with the inner-pipe and so as the rest of the zones. The boundary conditions of the outer pipe are kept same as that of the constant wall temperature. The bottom and top walls of the PCM domain are kept as adiabatic walls considering that there is no heat added or lost. It is considered that the LHTES system is at 298 K as the initial condition.

During the solidification case PCM, fins and inner-pipe are patched with a temperature of 395 K and the outer pipe at 389 K which is the average temperature obtained from the above melting case. Here we assigned the inlet and outlet boundaries as an adiabatic wall, considering that we close the stovepipe of the wood stove once combustion is over. By doing so we, minimize the heat losses through the pipe, and we patch the hot gas domain at 373 K. The boundary conditions of the walls of the PCM remain the same as that of the melting condition.

At the initial time, the PCM is taken to be a motionless solid or liquid which is maintained at constant temperature for both models.

5.3.2 Parameters for converged solution

With numerous studies and observations during the simulation, it was seen that certain values and parameters played an important role to reach a converged solution. Some of the important ones are listed below:

- **Density:** As the density of the PCM varies with increase or decrease in temperature during its melting and solidification process. The density was set as piece-wise linear function of temperature, considering the fact that FLUENT will take care of the density in the mushy zone.
- **Reference value:** It is important that the default reference values are set to the geometry and the values of PCM. Changes made on the reference values are: Area 0.03 m^2 , Density 1360 kg/m^3 , length 0.3 m, velocity 0.0001 m/s , viscosity 0.001067 kg/m-s , Temperature 298 K.
- **Melting ΔT range:** It was noticed that the temperature difference between the solid and liquid states of PCM played a huge role. At the beginning of the simulation, the temperature difference was maintained at 0.5 K to 2 K and it showed instability and very thin layer of the mushy zone. With a temperature difference of 3 K it showed a good stability, hence, it was decided to keep it for rest of the simulations.
- **Solution method:** PRESTO scheme is used for the pressure correction equation and a well-known Semi-IMPlicit Pressure-Linked Equation (SIMPLE) algorithm is used for the pressure-velocity coupling. Momentum, turbulent kinetic and energy equations were computed using the first-order scheme.
- **Relaxation factors and time step size:** These two are the most important parameters which had to be observed very closely. When default values of FLUENT were maintained in under relaxation-factors, solution never reached the convergence criteria. After several manipulations and trials, a standard values was yield which gave a converged solution. It was set to be Pressure 0.3, Density 0.8, Momentum 0.3, Body Forces 1, Liquid Fraction 0.1, Energy 0.9, Turbulent Kinetic Energy 0.8 and Turbulent Dissipation rate 0.8. In order to satisfy the convergence criteria, during the initial heating and cooling the

number of iterations for every time steps was 200 and it was reduced to 50-100 iterations once the solution converged. Sensitivity analysis has been done by varying the time step, it was found that 1 s is an appropriate time to accurately predict the behavior of the PCM during the melting process. But, it was noticed that 1 s of time step was not sufficient for the solidification case and a time step of 0.5 s gave the best results.

5.4 Determination of flow model

It is important to know which flow-model is best for the simulation. Using the correct model will give us faster convergence and more realistic solution. When an inner wall is maintained at constant temperature than there is no question of using any other flow-model apart from laminar viscous to solve the equations. However, the physics changes when we introduce a flow in the pipe, to determine if the flow is laminar or turbulent we first need to calculate its Reynolds number.

$$Re_D = \frac{\rho u D_h}{\mu} \quad (15)$$

Where Re_D is the Reynolds number for hydraulic diameter, u is the inlet mean velocity $1 \text{ (ms}^{-1}\text{)}$, D_h is the hydraulic diameter 0.15 (m) , ρ is density of hot air $0.72 \text{ (kg/m}^3\text{)}$, μ is dynamic viscosity $2 * 10^{-5} \text{ (kg/m-s)}$. Using the above values for hot gas the Reynolds number is:

$$Re_D = 4390.25$$

According to the literature [38], an internal flow is considered turbulent if the Reynolds number based on hydraulic diameter Re_D is greater than the critical value $Re_{D,crit}$. The critical Reynolds number for an internal flow is typically assumed to be $Re_{D,crit} = 2300$. Since, our Reynolds number is more than the critical value we have to go with a turbulent model.

Since we are using a turbulent model it becomes important which turbulent model is most suitable for our case. One of the factors that decides which model to use is the $y+$ value. In general, the $y+$ value for pipe ranges from 12 to 20 [38]. Hence, k-epsilon model is the most suitable one for our case. Assuming that the turbulent intensity is around 5% in the pipe we can calculate kinetic energy and dissipation rate and it is found to be $k = 0.375 \text{ (m}^2\text{/s}^2\text{)}$ and $\epsilon = 3.59 \text{ (m}^2\text{/s}^2\text{)}$ and the minimum wall distance Δs is 0.0054 mm.

6 Results and discussion

6.1 Effect of fin frequency on melting and solidification processes

Figure 18a shows the impact of fins presents in the PCM during its charging process. It is seen from the graph that PCM is never completely melted when there were no fin, 1 fin and 2 fins, even after heating the PCM for more than 5 hours. However, when there were 3 fins in the PCM block, heat transferred to the PCM was sufficient to melt the whole of PCM just within 140 min. From the graph it is also seen that for 90 % of melting time for 1 fin, 2 fins and 3 fins were 10.5 %, 21 % and 63 % faster than without fins. Hence, it was arrived to a conclusion having 3 fins for the 300 mm long pipe is the best for our case. A higher number of fins would give too much heat too quickly to the PCM, risking temperature over degradation temperature. More fins would also make the whole system heavier.

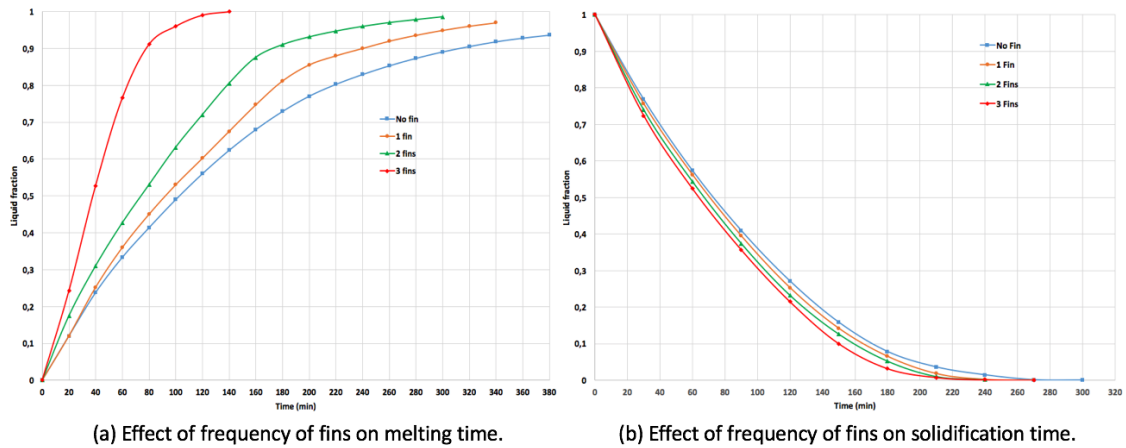


Figure 18: *Effect of fin frequency on melting and solidification processes.*

Figure 18b shows the solidification rate of PCM, the fin frequency does not have much of an effect during solidification processes as the liquid fraction curves are close by. Hence, it becomes evident that having 3 fins is the best case as it would take less time to melt and solidifies the PCM than with the other 3 cases.

Figures 19 & 20 show the CFD results of the study of the fin frequency during its melting and solidification processes after one hour of physical time. It is observed that with increment in the frequency of fins there is more volume of PCM melted or solidified for the same given amount of time. It is also observed from the no fin case that natural convection led to the faster melting rate at the upper part of the heat exchanger when compared to the bottom. Solidification case shows the opposite effect, there is faster solidification rate in lower part as compared to the top, is due to the effect of natural convection.

According to the results observed from frequencies of fins with constant wall temperature, it was clear enough to go on with three fins with the hot gas cases.

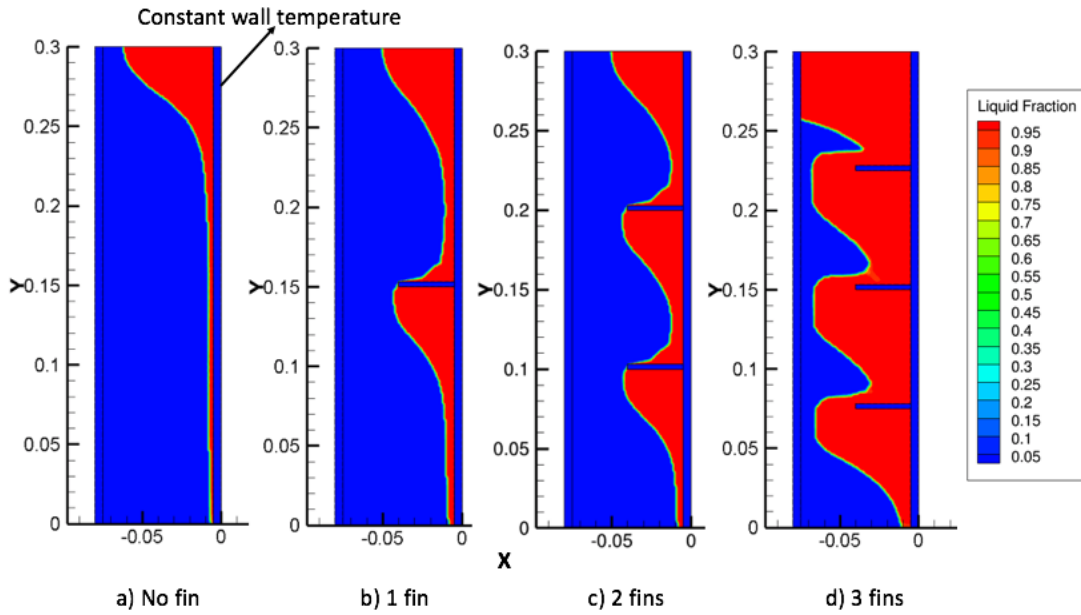


Figure 19: *CFD results of melting rate due to fin frequency for 35mm fins after one hour.*

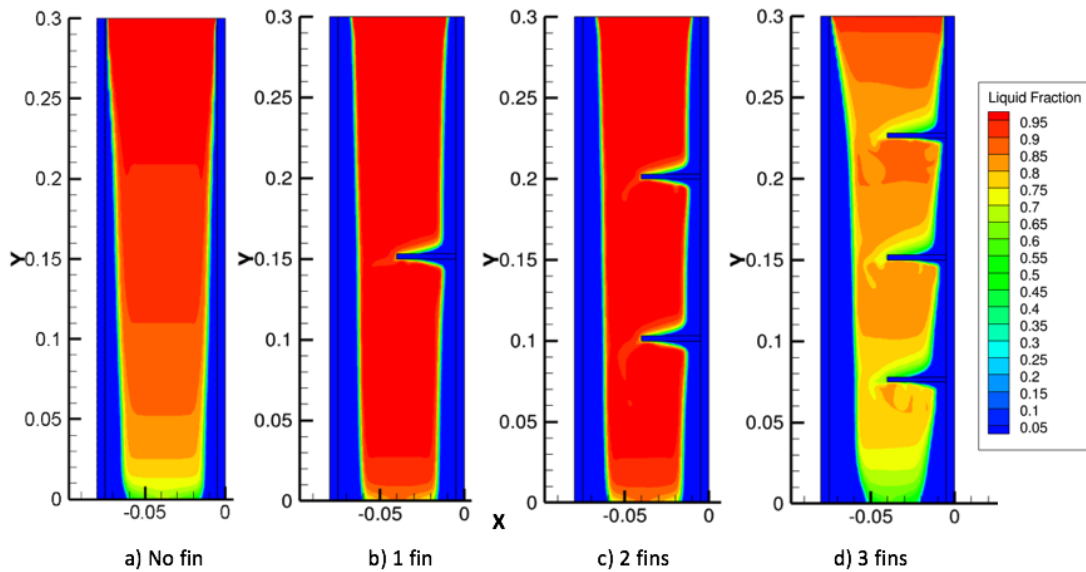


Figure 20: *CFD results of solidification rate due to fin frequency for 35mm fin after one hour.*

6.2 Effect of fin lengths on melting and solidification processes

It was observed that fin length played an important role during melting and solidification of the PCM in the heat exchanger. With the installation of fins it was possible to enhance the rate of heat transfer to the PCM, which directly affected the melting and solidification rate of the PCM.

As 3 fins showed the optimum result for melting and solidification processes in 300 mm long pipe, simulation for varying fin length will be performed for 3 fins case.

6.2.1 Constant wall temperature

Figure 21a shows the effect of fin length on the melting rate (liquid fraction) of the PCM for different cases. It can be seen that the PCM never fully melted with no fin present. However, with the presence of fins, the melting time of PCM decreased with increasing the fin length. 90 % of melting time for 17.5 mm, 35 mm, 52.5 mm and 70 mm fins were 57.8 %, 63.2 %, 68.4 % and 73.6 % faster than without fins. This is because the fins extend the heat transfer area to the PCM surface.

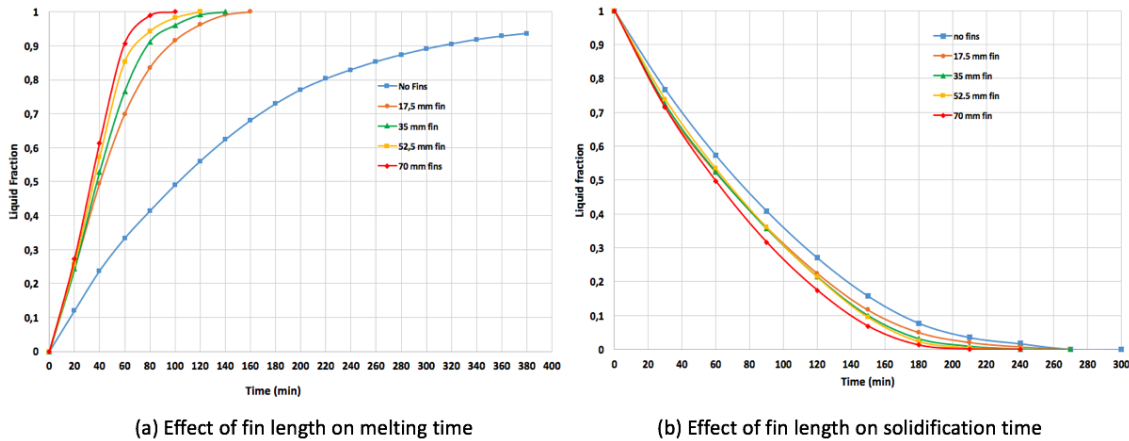


Figure 21: *Effect of fin length on melting and solidification process.*

Figure 21b shows the solidification rate of the PCM with fins. Here we observed that the solidification process is the slowest for no fin case. The solidification for 70 mm fins is the fastest, meaning more heat is extracted to the surrounding. However, 17.5 mm, 35 mm and 52.5 mm fins have relatively similar curve during the process of solidification. This is due to the fact that there is no on the cold side of the PCM. In addition, since the solidification is conduction-driven, the presence of the fins on the right side dose not affect much of the solidification.

Figures 22 & 23 show the liquid fraction for melting and solidification. In the melting process, we can see that introducing fins can directly affect the melting rate. One more observation that we can make from here is that increasing fin length may not necessarily increase the melting rate. As we see that melted volume in the 70mm fin case is less than that of the 35 mm fin case. This is because the heat transport through natural convection is blocked by the fins in the 70 mm case.

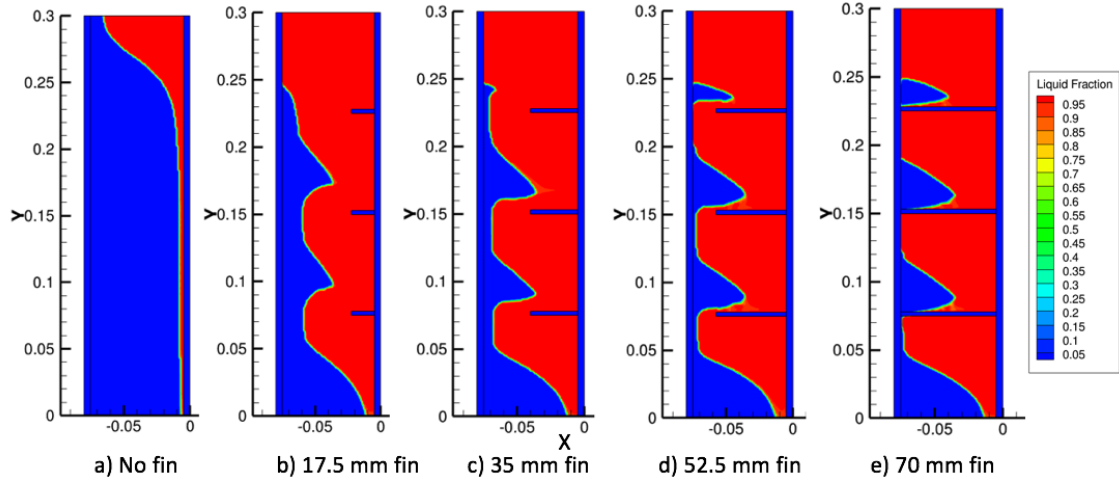


Figure 22: *CFD results of fin length on melting process after one hour.*

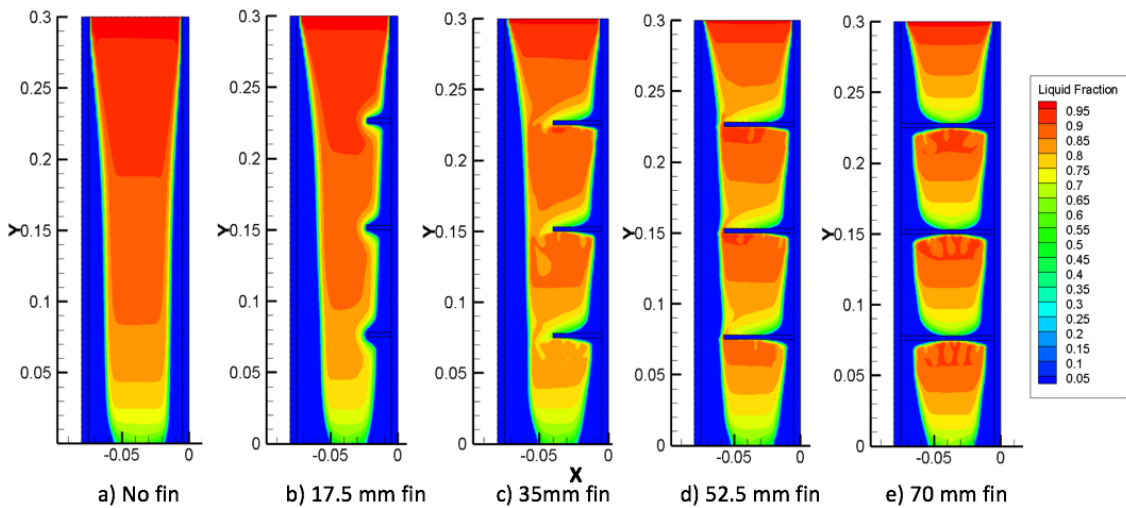


Figure 23: *CFD results of fin length on solidification process after one hour.*

6.2.2 Hot gas flowing in the stovepipe with an inlet temperature of 498 K

In the melting case, hot gas with 498 K is introduced at the inlet of stovepipe with a constant velocity of 1 m/s. Here it is assumed that heat is transferred from the hot gas to the inner pipe wall then eventually to the PCM. For the solidification case, the inlet and outlet are assigned as an adiabatic wall to simulate the closing of a valve on top and bottom of the stovepipe, leading to a reduction of the heat losses back to the inner pipe.

Figure 24a shows the liquid fraction during the melting process for different fin lengths. It is observed that it takes considerably longer to melt the PCM as compared to the previous case with constant wall temperature. It was possible to melt the PCM completely for the 70 mm fin case only after heating it for 11.5 hours. It can also be observed from the graph that the liquid fraction for the 70 mm fin case lies below other finned cases until 5 hours of heating. This is due to the restriction

of movement of the melted PCM, hence, there is no heat transport by natural convection in the other blocks of PCM. The 52.5 mm fin case has a very similar effect as that of 70 mm fin. It is seen from the figure that the case with no fin hardly manages to reach a liquid fraction 0.7.

From the curve of the 17.5 mm and 35 mm fins cases, it is seen that the liquid fraction reaches 0.9 within 4 hours of heating. However, as the heating progresses, the liquid fraction decreases instead of following the expected increasing trend. This effect is due to the presence of natural convection. Hot melted PCM is transported through buoyancy to the top while the cooler melted PCM is transported to the bottom, eventually creating a sufficient vertical temperature gradient to cool down the lower part PCM block under melting temperature. This effect is amplified by the continuous exchange of heat between the melted PCM and the outer pipe which is exposed to ambient temperature of 298 K.

Figure 24b shows the solidification process for the different finned lengths cases and the no fin case. In these cases, we assume as a starting condition that PCM present in the heat exchanger is completely melted and has a temperature of 395 K. During the process of discharging, it is seen that the 70 mm fin case solidifies significantly faster than the other cases. There, the PCM is completely solidified after 5.5 hours, followed by the 52.5 mm fin case with a solidification time of 6.5 hours. The no fin and 17.5 mm fin cases show a very similar rate of solidification. It is seen that the 35 mm fin case has the lowest solidifying rate as it takes around 9.5 hours to completely solidify the PCM.

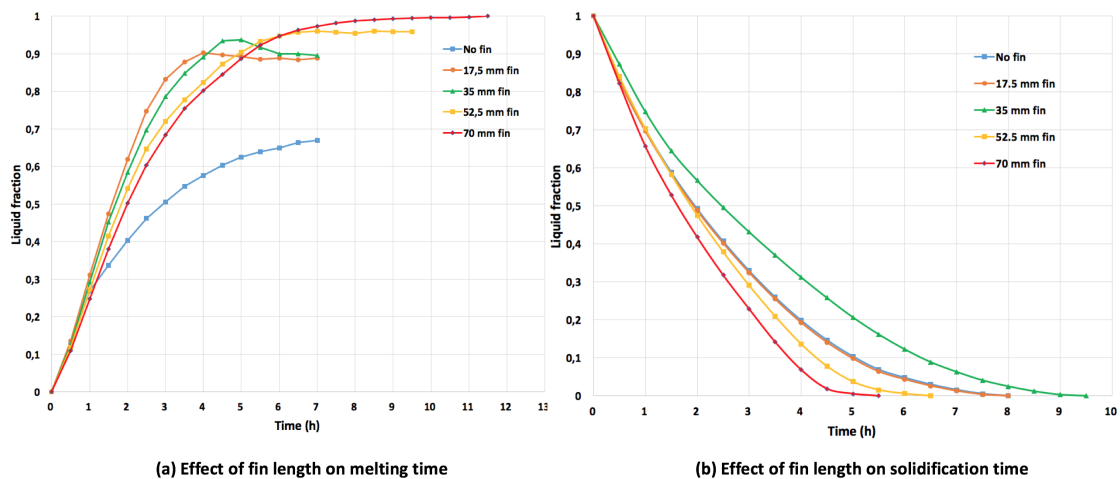


Figure 24: *Effect of fin length on melting and solidification processes for hot gas inlet with 498 K.*

To have a more realistic simulation, a dynamic plot for melting and solidification processes is shown in Figure 25. Here it is considered that the system is heated for 6 hours until the boundary conditions in the inner pipe are changed to trigger the PCM discharge. 6 hours of heating corresponds to a realistic wood stove combustion cycle with several batches. Here the temperature of the hot gas is kept constant

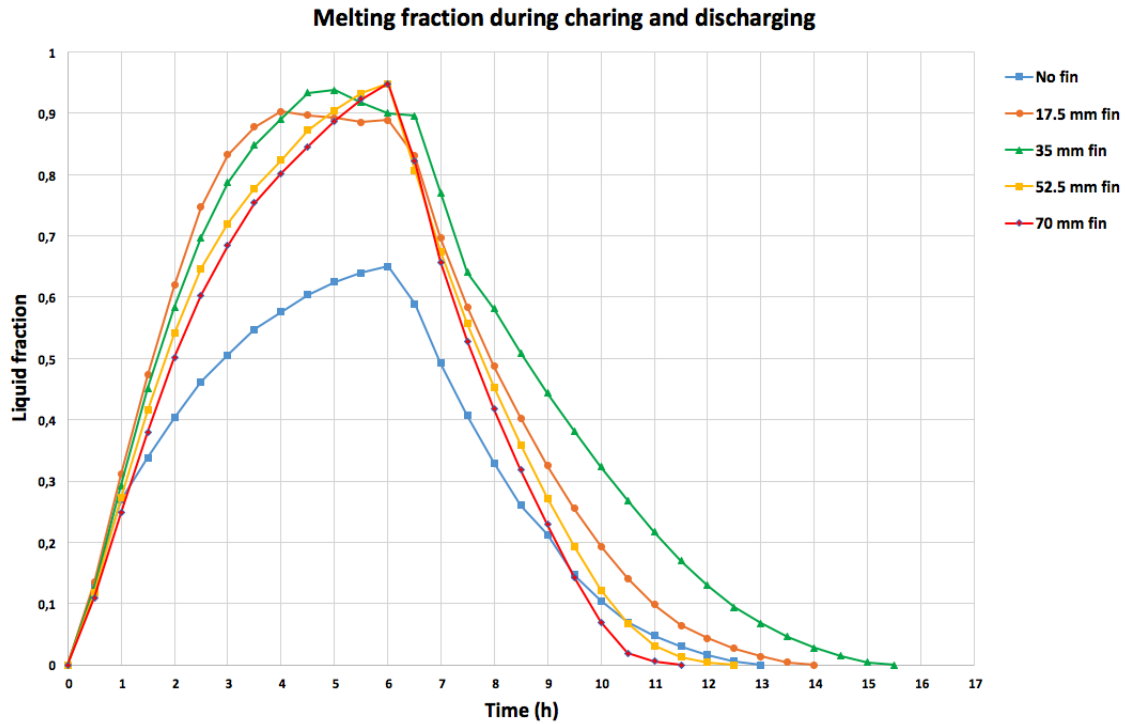


Figure 25: Effect of fin length on melting and solidification processes for hot gas inlet with 498 K for dynamic case.

to 373 K at the stovepipe inlet to simplify. It is seen from the graph that the 17.5 mm, 35 mm, 52.5 mm and 70 mm finned cases reach a liquid fraction of 0.9 by 6 hours, whereas the no fin case reaches a liquid fraction of 0.65. Over the charging time for finned cases, it is seen again that natural convection has a strong influence over the melting, as stated in the previous section. Though the fraction of melted PCM is higher for the 52.5 mm and 70 mm finned cases during the charging process, it also solidifies at a faster rate when compared to the 35 mm fin case as there is higher heat exchange. Since our goal of the concept is to achieve a slow but close to complete melting to avoid overheating the PCM and release the stored heat over 6 to 10 hours, it can be concluded that 35 mm is the best-finned case for our study.

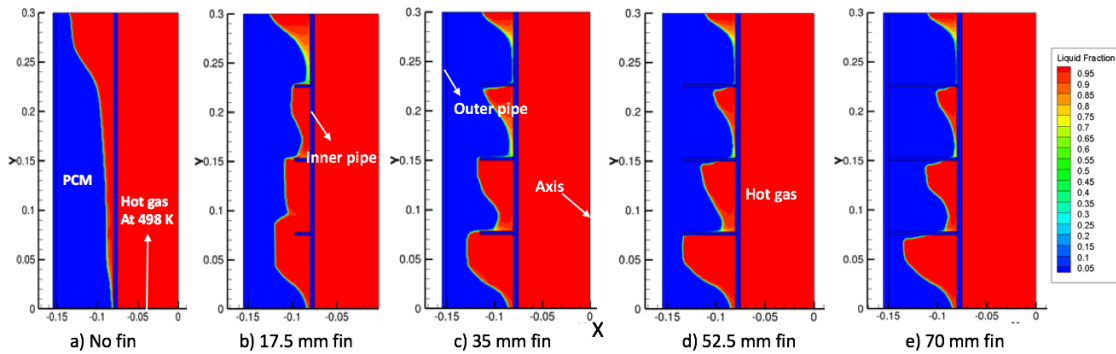


Figure 26: CFD results for melting after one hour for different cases with hot.

Figures 26 & 27 show the CFD results of PCM melting and solidification after one hour for all the cases. It is seen that. However, more PCM is melted on the upper part of the heat exchanger for the no fin case. This is because the melted hot PCM circulates due to the presence of natural convection driven by buoyancy. Like the constant wall temperature cases, the melted PCM volume is less in the 70 mm finned case compared to the 35 mm finned case.

For the solidification process in Figure 27, it is seen that the solidification rate for 70 mm fins is significantly higher as compared to the other cases. It is seen that the solidification process progresses logically from the outer pipe wall since it is in contact with the surrounding maintained at 298 K.

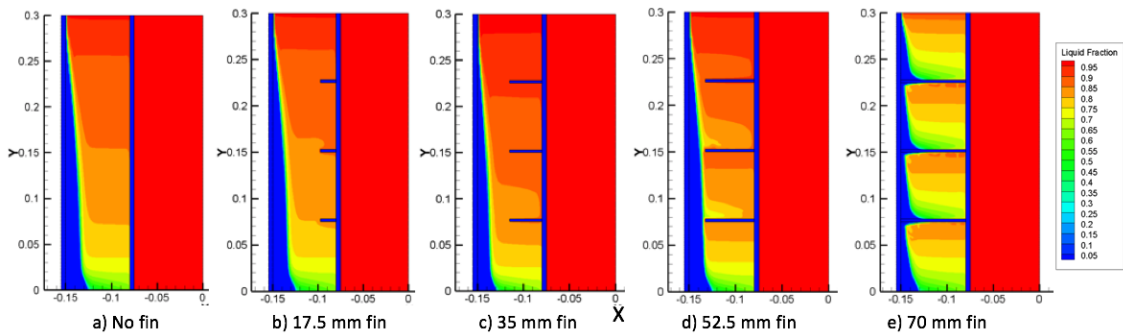


Figure 27: *CFD results for solidification after one hour for different cases with hot gas.*

6.3 Temperature variation on the outer pipe wall

6.3.1 Constant wall temperature

It is considered that there is constant heat supply of 415 K for 3.5 hours through the inner pipe wall during charging then it is made to discharge by changing the boundary condition of the inner pipe wall. Figure 28 shows the variation of temperature in outer pipe wall during charging and discharging of the PCM. It can be seen that the outer wall reaches a temperature above the melting temperature of PCM (391 K) as the PCM present in the heat exchanger is completely melted except for the no fin case. It is also seen that temperature remains constant on the outer pipe once the PCM is completely melted during the charging process. In the initial process of discharging 70 mm fin shows a relatively higher temperature compared to rest of the fin case, this is because there is direct contact between the 70 mm fin and outer pipe. Hence, there is more supply of heat to the outer pipe during discharge of PCM. From the graph, it is observed that it takes around 7.5 hours to decrease to its initial temperature of 298 K, which is two times more than that of charging time.

Figure 29 shows the temperature distribution after one hour of melting for all the cases; it is clear from the figure that PCM in 70 mm fin case reaches the highest temperature for the same given time. It can also be observed that the melted PCM

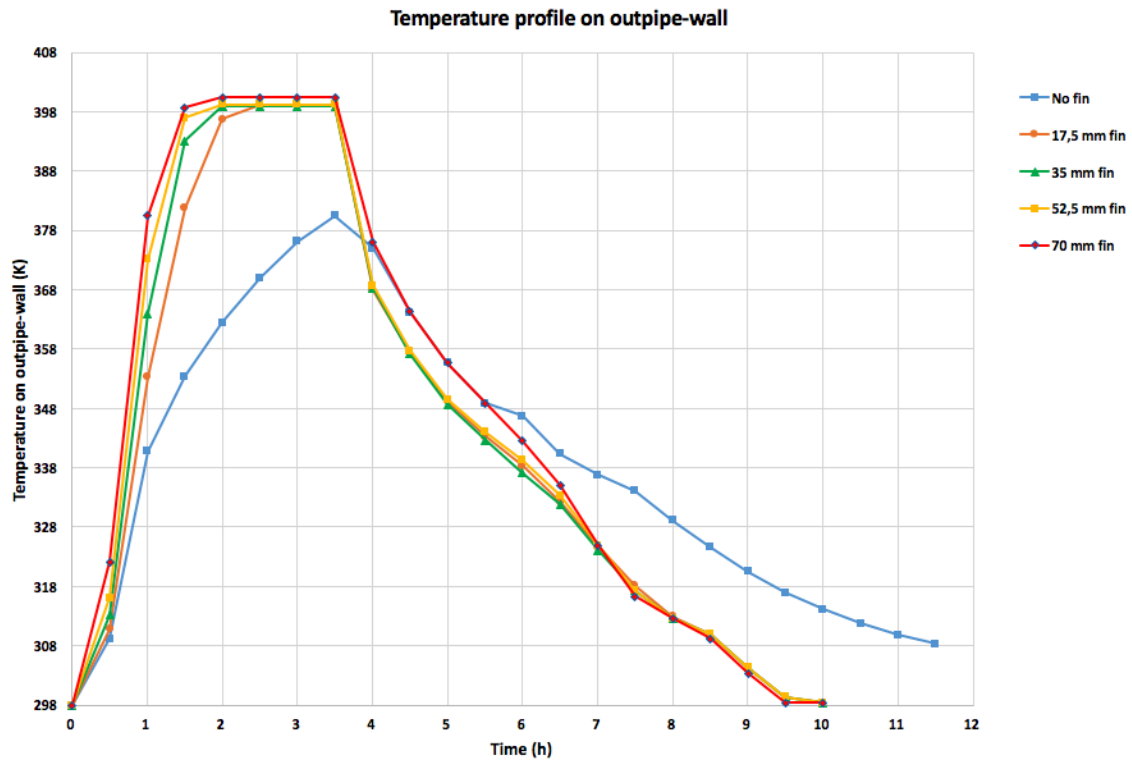


Figure 28: Variation of temperature on out pipe-wall during charging and discharging of PCM

on the left side of the fins has higher temperature compared to the right side of the fins. This effect is due to the presence of natural convection in the melted fluid. However, in the case of no fin, we see that only a small portion of the PCM reaches a temperature higher or equal to melting temperature of PCM. This is because there is no extra surface to enhance the heat distribution to the PCM apart from the inner pipe wall, hence the overall temperature in no fin case is relatively lower.

Figure 30 shows the temperature distribution after one hour of solidification process for all the cases; temperature in PCM is decreased faster with the longest fins length. PCM closer to the fins and the pipes get cooler faster than rest of the part as there is higher heat transfer. It can be seen that 70 mm case cools down faster compared to the rest as there is direct contact between the inner and outer pipe, hence higher heat exchange between the PCM and the surrounding. It is seen that PCM near the outer pipe cools down faster compared to the inner pipe, this is because the outer pipe is exposed to an ambient temperature of 298 K while the inner pipe is maintained at 323 K.

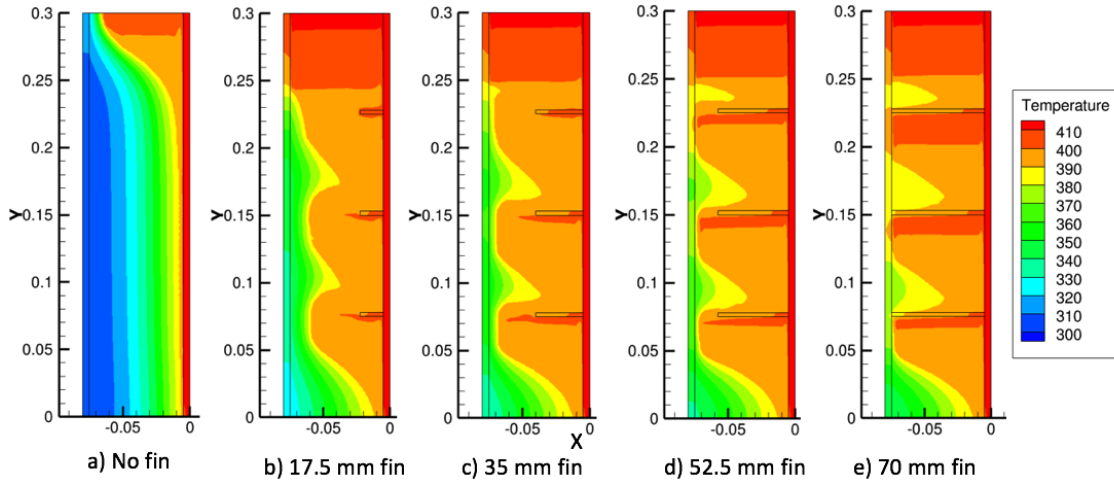


Figure 29: *CFD results for variation of temperature in heat exchanger during melting process after one hour.*

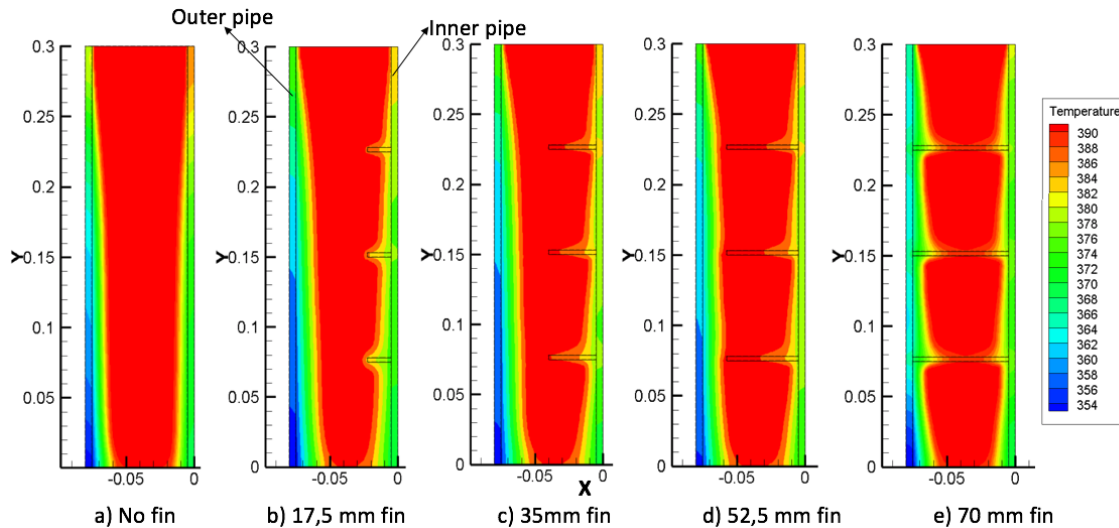


Figure 30: *CFD results for variation of temperature in heat exchanger during solidification process after an hour.*

6.3.2 Hot gas flowing in the stovepipe with an inlet temperature of 498K

The temperature range in the outer pipe wall is dependent on how much heat is absorbed or released by the PCM during the processes of charging and discharging. Figure 31 shows the temperature profile in the outer pipe wall during PCM charging and discharging. It is considered that heat is supplied to the PCM through stovepipe inlet at 498 K for 6 hours then it is bound to discharge by changing the boundary conditions. From the graph, it is observed that, in the 70 mm finned case, the outer pipe wall is heated up faster and reaches highest temperature compared to the other cases. This is because there is direct contact between the inner pipe (heated with hot gas) and the outer pipe through the steel fins. However, it is seen that the outer pipe does not reach the temperature of the inner pipe as shown in the graph. This

is because of the heat absorbed by the PCM through the melting process.

It can also be seen that the 35 and 52.5 mm finned case have a very similar temperature profile until 5 hours of charging where there is a further increment in temperature for the 52.5 mm finned case as there is less room for natural convection to occur in the PCM. Whereas for the 35 mm finned case, the temperature decreases due to the presence of natural convection and continuous heat exchange with the surrounding. It is also seen from the graph that for the 17.5 mm finned case, the temperature becomes constant after 4 hours of heating. During the process of discharge, it is again seen that 70 mm fin case dominates the other cases for a while as the temperature was higher at the start of the discharge but eventually releases heat faster than most other cases.

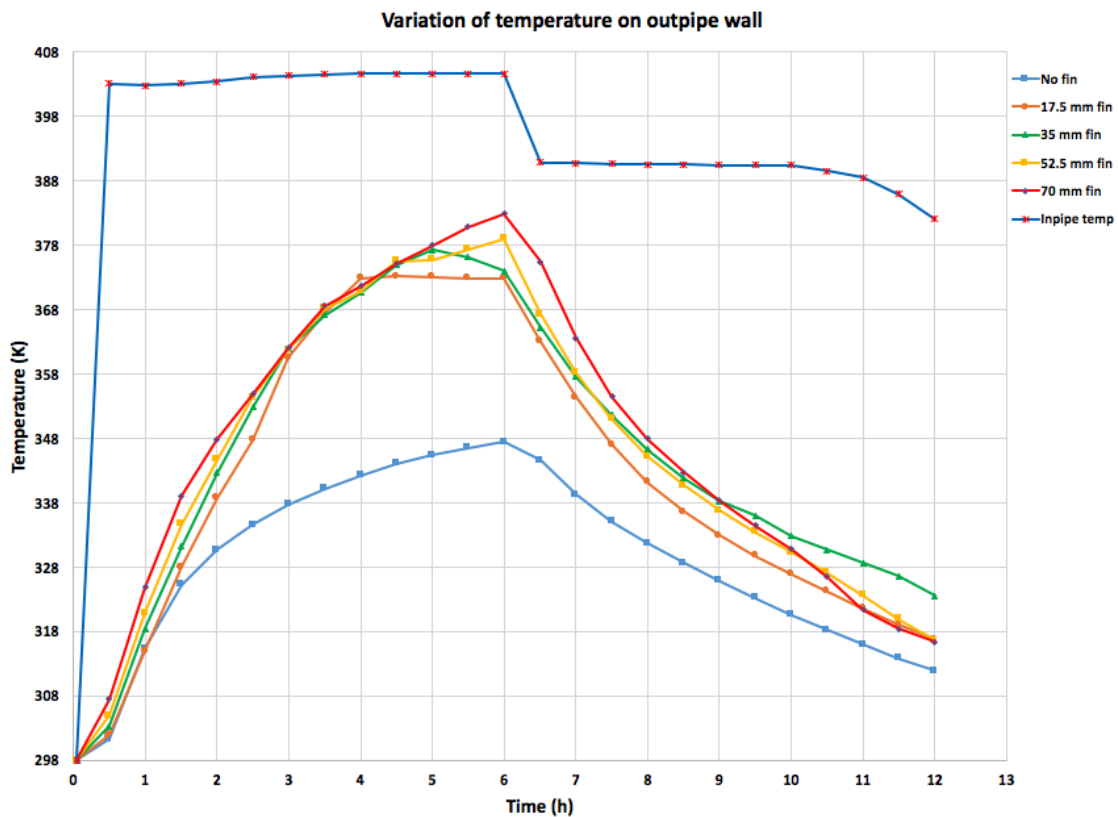


Figure 31: Variation of temperature on out pipe-wall during charging and discharging for hot gas

Figures 32 & 33 show the temperature fields during PCM melting and solidification processes after one hour of physical time. From the melting cases, it is clearly seen how fins can enhance the heat transfer to the PCM as well as how the heat transfer to the PCM is in all cases driven by convection. For the solidification case, it is observed that all the cases have relatively similar temperature profiles for the first hour of discharging except for the 70 mm fin case. Since there is direct contact between the fins and the outer pipe, there is higher heat transfer rate for 70 mm fin case to the outer pipe.

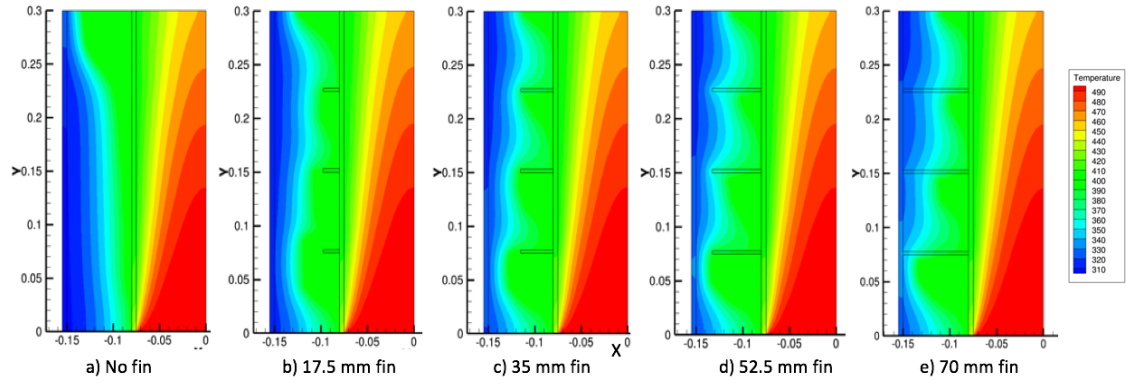


Figure 32: *CFD temperature profile for different fin cases for melting process after one hour with hot gas at 498 K.*

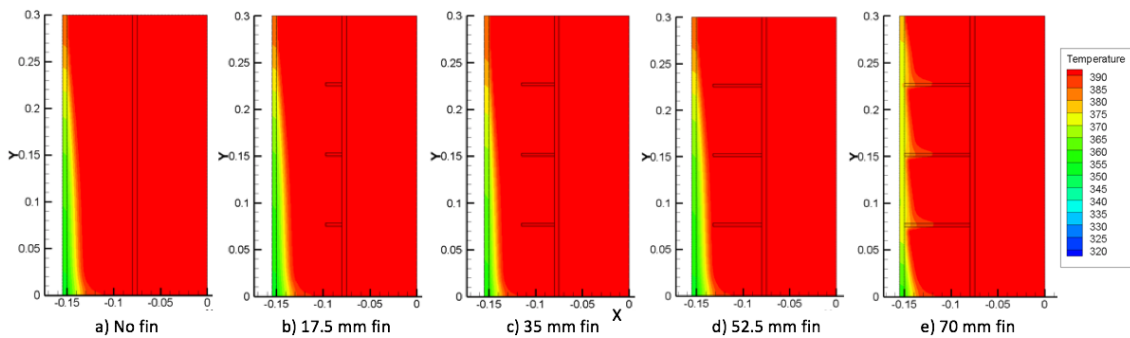


Figure 33: *CFD temperature profile for different fin cases for solidification process after one hour with inlet and outlet as adiabatic walls.*

6.4 Heat given to the PCM and heat transfer to the outer pipe

Figure 34 shows the heat transferred to the PCM from the inner pipe and the heat transferred from the PCM to the outer pipe (in contact with the surrounding). Here it is considered that the PCM is heated for 6 hours, then it is bound to discharge by changing the boundary conditions in the simulation.

From the graph, it is observed that the 70 mm fin case reaches a thermal balance after 5 hours of heating the PCM as the curve intersects. However, when the heating is further continued for another hour, it is seen that more heat is extracted to the outer pipe than supplied to the PCM. This phenomenon occurs because the fins are in direct contact between the inner pipe and outer pipe, which increases the heat transfer excessively since the fins (steel) have a 98.5 % higher conductivity as compared to liquid PCM (erythritol). This resulted in an excessive loss of heat to the surrounding, starting the discharging of the PCM before it is needed. For the 35 mm fin case, it nearly reaches a thermal balance after heating the PCM for 5 hours, but with another hour of heating, more heat is being absorbed by the PCM and less heat is supplied to the surrounding from the outer pipe. Over the course of heating the PCM, it was observed that the PCM in the lower portion of the heat

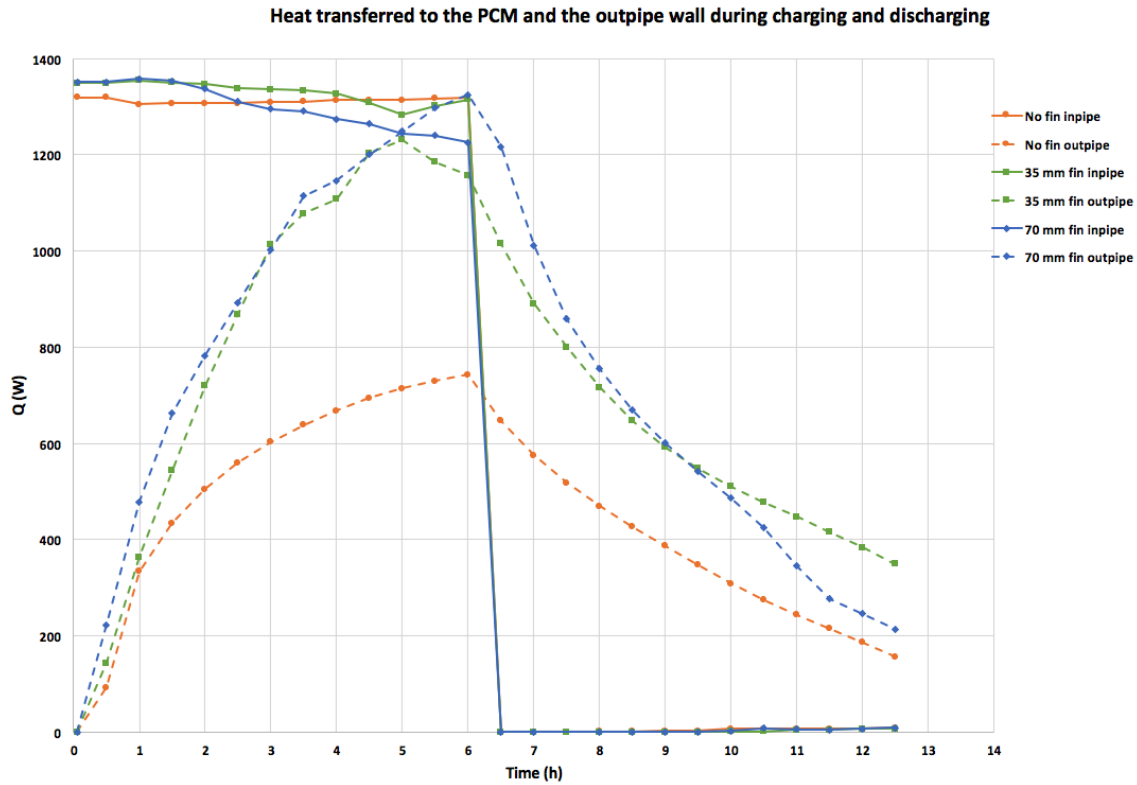


Figure 34: Variation of heat supplied to the PCM and the outpipe.

exchanger was starting to solidify due to the heat transfer to the outer pipe. From the graph, it is seen that for the no fin case, it would take hours of heating to reach a thermal balance.

The drastic change in heat supplied to the inner pipe or the PCM is due to the change in boundary conditions to trigger the solidification process. It is observed that there is a minor loss of heat from the inner pipe during the process of solidification for all the cases towards the end of the solidification process. For the 70 mm finned case, it is seen that the heat is released at a faster rate to the surrounding during the solidification process, whereas the 35 mm finned case releases the heat moderately slower. The no fin case does release the heat in a prolonged manner, but there is not much heat release from the PCM as it was not fully melted. Hence, the 35 mm finned case shows the best results out of all the cases considering the requirements of the concept. It is seen that the solidification is complete after 12.5 hours though there is still energy in the PCM to supply to the surrounding (sensible heat).

6.5 Variation of temperature in PCM during charging and discharging

Figure 35 represents the mass-weighted average temperature profile in the PCM during the processes of melting and solidification in the heat exchanger. It can be seen that all the finned cases have a similar temperature profile for the first 2.5 hours

of heating. Then it is seen that for the rest of charging time, the PCM temperature for the 70 mm finned case keeps on increasing. It can be seen that in the case of the 52.5 mm fins, there is a fluctuating temperature. This was due to the restriction in movement of the melted PCM in the heat exchanger as there is only a tiny gap between the fins and outer pipe wall. It can be seen that the 17.5 mm and 35 mm finned cases show a very similar behaviour as there was more room for the melted PCM to circulate inside the heat exchanger. However, for the no fin case, the PCM hardly manages to reach a higher temperature as there is no extended surface to the PCM apart from the inner pipe wall.

During the discharge process, it is observed that the 70 mm finned case has a higher average temperature in the initial stage of discharge. After 10 hours, there is a sudden drop in temperature. This situation also applies to the 52.5 mm finned case. The reason is that as the PCM solidifies it gains a higher conductivity which in turn increases the heat transfer to the outer pipe. As it was stated in the previous section, the PCM starts to solidify from the outer pipe wall. Therefore, once this PCM solidifies and comes in contact with the fins, it starts to extract the heat from the PCM at a faster rate. Hence there is a sudden drop in PCM temperature.

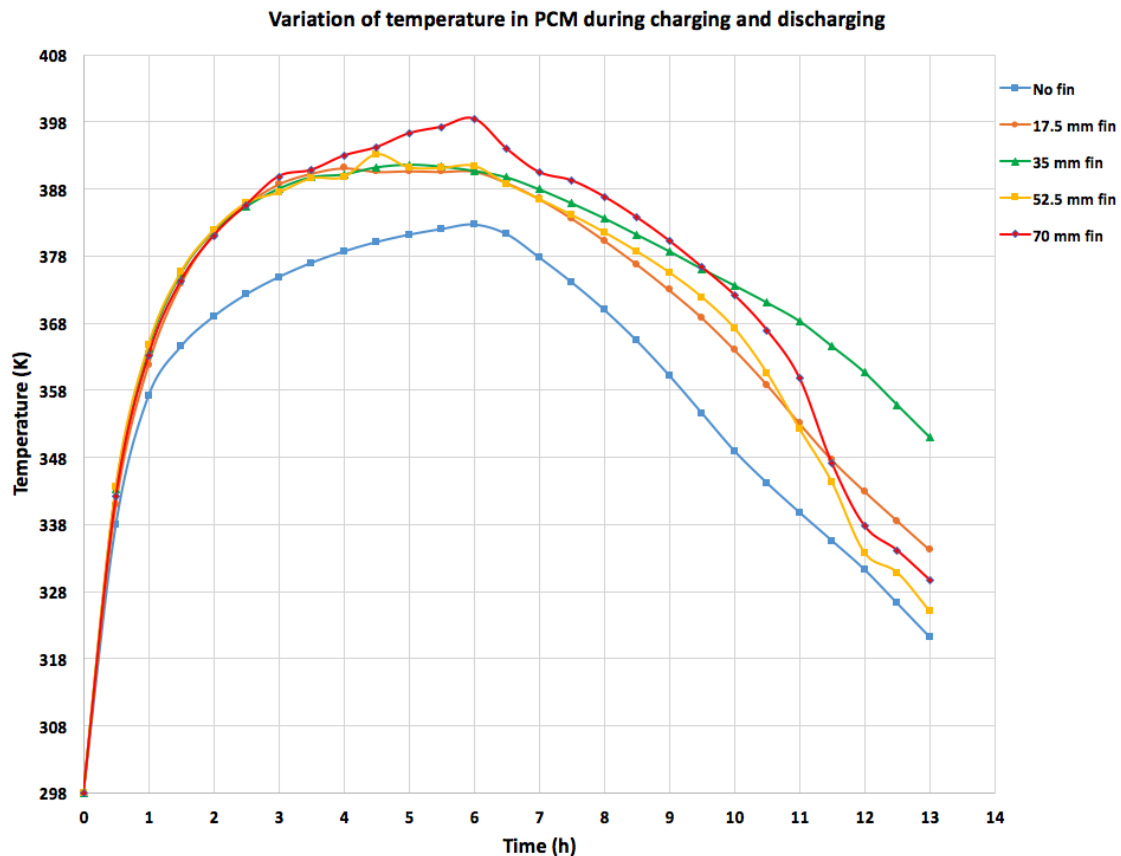


Figure 35: variation of temperature in PCM during charging and discharging

Hence, by now with all the observation made, it is possible to conclude that having 35 mm fins for this configuration provided a better solution.

7 Conclusion and recommendations

A review of latent heat storage system and modeling the system has been studied to understand the working principle of it. Two models have been developed for a vertical stovepipe energy storage system with PCM, constant wall temperature system and hot gas system. CFD simulation was performed on these models to understand the behavior of PCM during its melting and solidification processes.

This work mainly focuses on the influence of frequencies of fins, the effect of fin lengths on melting and solidification of the PCM, natural convection in PCM, and thermal behavior of the PCM. It was observed that with increasing frequencies of the fin in the volume of PCM it melted the PCM faster, for 90 % of melting time for 1 fin, 2 fins and 3 fins were 10.5 %, 21 % and 63 % faster in melting time than without fins. However, it did not show much of influence during the process of solidification as there was no fin attached to the outer pipe. It was also observed that the fin lengths had a huge influence on the rate of melting of the PCM. For the constant wall temperature case it was seen that 90 % of melting time for 17.5 mm, 35 mm, 52.5 mm and 70 mm fins were 57.8 %, 63.2 %, 68.4 % and 73.6 % faster than without fins. However, for the hot gas case, it did show a slightly different result as the heat applied to the PCM was a varying temperature along the inner pipe and also due to the strong effect of natural convection. After close observation, it was seen that 35 mm fin case provided the best result for melting as well as for solidification processes. It was seen that during the discharge (solidification) process the phase change starts from the bottom and ends at the top of the heat exchanger. In contrast during the charging (melting), process phase change commences from the top and ends at the bottom. It was found that the melting phase change duration is quicker compared to the solidification process due to the effect of natural convection and finned surfaces. It was observed that temperature profile on the outer pipe wall was constant after 2 hours and remained constant for the rest of the charging time for constant wall temperature. However, for the hot gas case, it was seen that the temperature on outer pipe wall kept increasing even after 6 hours of charging as the PCM in heat exchanger was not melted completely. One more interesting observation was made over the process of melting the PCM, as the heating progresses after 5 hours the liquid fraction decreases instead of increasing. This effect is due to the presence of natural convection. Hot melted PCM is transported through buoyancy to the top while the cooler melted PCM is transported to the bottom, eventually creating a sufficient vertical temperature gradient to cool down the lower part PCM block under melting temperature. This effect is amplified by the continuous exchange of heat between the melted PCM and the outer pipe which is exposed to ambient temperature of 298 K.

It was observed that for 70 mm finned case the heat given to the PCM was less than heat given out of outer pipe after 5 hours of heating in hot gas case. This phenomenon occurs because the fins are in direct contact between the inner pipe and outer pipe, which increases the heat transfer excessively since the fins (steel) have a 98.5 % higher conductivity as compared to liquid PCM (erythritol). This

resulted in an excessive loss of heat to the surrounding, starting the discharging of the PCM before it is needed. However, 35 mm finned case had a stable thermal balance between the heat inputted to the PCM and heat going out of outer pipe. It was also observed that during the process of discharging 35 mm finned case releases the heat moderately slower than other finned cases. Hence, the 35 mm finned case shows the best results out of all the cases considering the requirements of the concept.

Recommendations for future work:

- The observation made from this CFD simulation are believed to be sufficiently reliable. However, it would be interesting to performed experiment to justify the effect of solidification during the course of charging.
- It would be interesting to look at 3D model simulation to understand the effect of vertical fins in the PCM.
- It would also be wise to reduce the thickness of the PCM and perform the simulation, to overcome the solidification process during charging.
- Different design of the heat exchanger should also be taken into consideration to increase the efficiency.
- Dynamic batch cycle simulation should be run to understand how PCM would react after a course of the period.

References

- [1] A.A. Al-Abidi, Sohif Mat, K. Sopian, M.Y. Sulaiman. *"Internal and external fin heat transfer enhancement technique for latent heat thermal energy storage in triplex tube heat exchanger"*. Applied Thermal Engineering, 2013.
- [2] Saleh Almsater, Alemu Alemu, Wasim Saman, Frank Bruno. *"Development and experimental validation of a CFD model for PCM in a vertical Triplex tube heat exchanger"*. Applied Thermal Engineering, January 2017.
- [3] Kolbeinn Kristjansson, Erling Næss, Øyvind Skreiberg. *"Damping of wood batch combustion heat release using a phase change material heat storage: Material selection and heat storage property optimization"*. Energy 115 378-385, Science Direct, 2016.
- [4] Atul Sharma, V.V Tyagi, C.R. Chen, D. Buddhi. *"Review on thermal energy storage with phase change materials and applications"*. Renewable and Sustainable energy Reviews 318-345 Science Direct, 2007.
- [5] Yvan Dutil, Daniel R.Rousse, Nizar Ben Salah, Stéphane Lassue, Laurent Zalewski. *"A review on phase-change materials: Mathematical modelling and simulations"*. Renewable and Sustainable Energy Reviews, 2010.
- [6] Alexis Sevault, Hanne Kauko, Mette Bugge, Krzysztof Banasiak, Nils Erland Haugen, Øyvind Skreiberg. *"Phase Change Materials (PCM) for thermal energy storage: state-of-the-art."* SINTEF Energy Research, project PCM-Eff, Inpress.
- [7] Ali Cherom Kheirabadi, Dominic Groulx. *"The Effect of the Mushy-Zone constant on Simulated Phase Change Heat Transfer"*. ResearchGate, 2015.
- [8] Voller VR. *"Fast implicit finite difference method for the analysis of phase change problems"* . Numerical Heat Transfer Part B 1990;17:155-69
- [9] Davide Lora. *"Phase change material product design. Market and business development assessment in the food industry"* . Teécnico Lisboa july 2014
- [10] Atul Sharma, S.D Sharma and D Buddhi. *"Accelerated thermal cycle test of acetamide, stearic acid and para n wax for solar thermal latent heat storage applications"* . In: Energy Conversion and Management 43.14 (2002), pp. 1923–1930.
- [11] Ahmet Sari. *"Eutectic mixtures of some fatty acids for low temperature solar heating applications: ermal properties and thermal reliability"* . In: Applied ermal Engineering 25.14–15 (2005), pp. 2100–2107.
- [12] D. Feldman, M.M. Shapiro, D. Banu and C.J. Fuks. *"Fatty acids and their mixtures as phase-change materials for thermal energy storage"* . Solar Energy Materials 18.3–4 (1989), pp. 201–216.
- [13] H. Mehling and L.F. Cabeza. *"Heat and cold storage with PCM: An up to date introduction into basics and applications"* . Heat and Mass Transfer. Springer, 2008.

- [14] Nihal Sarier and Emel Onder. "Fatty acids as phase change materials: A review". *Thermochimica Acta* 540 (2012), pp. 7–60.
- [15] Yanping Yuan, Nan Zhang, Wenquan Tao, Xiaoling Cao and Yaling He. "Organic phase change materials and their textile applications: An overview". *Renewable and Sustainable Energy Reviews* 29 (2014), pp. 482–498.
- [16] Zhi Ying Zhang and Meng Lin Yang. "Heat capacity and phase transition of 2-amino-2-methyl- 1,3-propanediol from 280 K to the melting point". *Thermochimica Acta* 169 (1990), pp. 263– 269.
- [17] Nihal Sarier and Emel Onder. "Organic phase change materials and their textile applications: An overview". *Thermochimica Acta* 540 (2012), pp. 7–60.
- [18] Zhi Ying Zhang, Meng Lin Yang and Hua Ping Li. "Heat capacity and phase transitions of mixtures of neopentylglycol and pentaerythritol from 270 K to their melting points". *Thermochimica Acta* 202 (1992), pp. 105–112.
- [19] Haiyan Feng, Xiaodi Liu, Shumei He, Kezhong Wu and Jianling Zhang. "Studies on solid–solid phase transitions of polyols by infrared spectroscopy". *Thermochimica Acta* 348.1–2 (2000), pp. 175–179.
- [20] Nasiru I. Ibrahim, Fahad A. Al-Sulaiman, Saidur Rahman, Bekir S. Yilbas, Ahmet Z. Sahin. "Heat transfer enhancement of phase change materials for thermal energy storage applications: A critical review". *Renewable and Sustainable Energy Reviews* 74 (2017) 26–50.
- [21] Ahmed Elgafy and Khalid Lafdi. "Effect of carbon nanofiber additives on thermal behavior of phase change materials". *Carbon* 43.15 (2005), pp. 3067–3074.
- [22] Comini G, Del Giudice S, Lewis RW, Zienkiewicz OC. "Finite element solution of non-linear heat conduction problems with special reference to phase change". *Int J Numer Methods Eng* 1974;8:613–24. <http://dx.doi.org/10.1002/nme.1620080314>.
- [23] Zeng X, Faghri A. "Temperature-transforming model for binary solid–liquid phase- change problems". part ii: numerical simulation. *Numer Heat Transf Part B Fundam* 1994;25:481–500. <http://dx.doi.org/10.1080/10407799408955932>.
- [24] Ozisik M Necati. "Finite difference methods in heat transfer". Florida: CRC Press.
- [25] Costa M, Buddhi D, Oliva A. " Numerical simulation of a latent heat thermal energy storage system with enhanced heat conduction". *Energy Convers Manag* 1998;39:319–30
- [26] Fang M, Chen G. " Effects of different multiple PCMs on the performance of a latent thermal energy storage system". *Appl Therm Eng* 2007;27:994–1000.

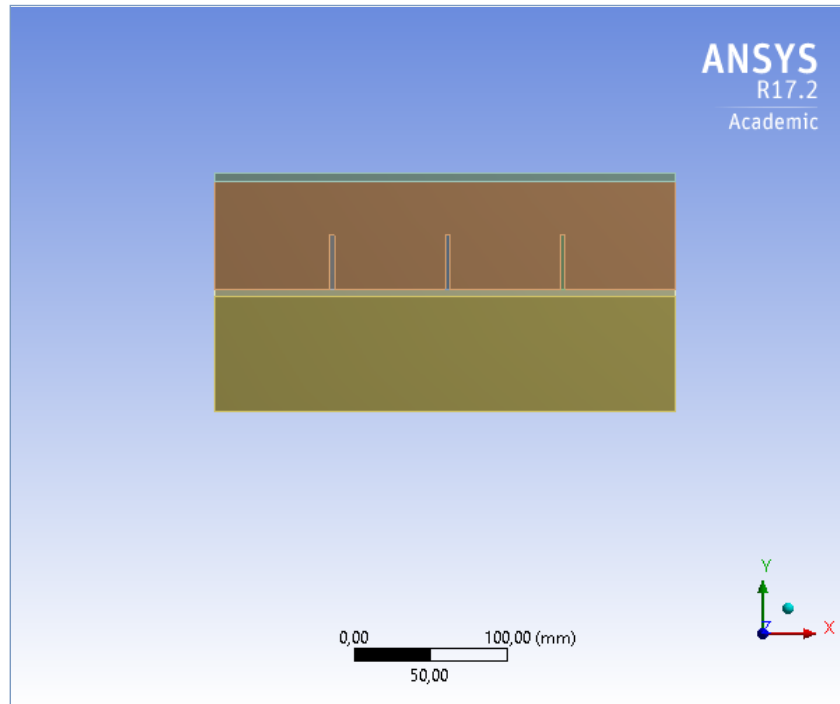
- [27] Gong Z-X, Mujumdar AS. " *Cyclic heat transfer in a novel storage unit of multiple phase change materials*" . Appl Therm Eng 1996;16:807–15.
- [28] Chen J, Yang D, Jiang J, Ma A, Song D. " *Research progress of phase change materials (PCMs) embedded with metal foam (a review)*" . Procedia Mater Sci 2014;4:389–94.
- [29] Siahpush A, O'Brien J, Crepeau J. " *Phase change heat transfer enhancement using copper porous foam*" . J Heat Transf 2008;130:82301.
- [30] Mettawee EBS, Assassa GMR. " *Thermal conductivity enhancement in a latent heat storage system*" . Sol Energy 2007;81:839–45
- [31] Cui Y, Liu C, Hu S, Yu X. " *The experimental exploration of carbon nanofiber and carbon nanotube additives on thermal behavior of phase change materials.*" . Sol Energy Mater Sol Cells 2011;95:1208–12.
- [32] Fukai J, Kanou M, Kodama Y, Miyatake O. " *Thermal conductivity enhancement of energy storage media using carbon fibers.*" . Energy Convers Manag 2000;41:1543–56.
- [33] Fukai J, Hamada Y, Morozumi Y, Miyatake O. " *Effect of carbon-fiber brushes on conductive heat transfer in phase change materials.*" . Int J Heat Mass Transf 2002;45:4781–92.
- [34] Fukai J, Hamada Y, Morozumi Y, Miyatake O. " *Improvement of thermal characteristics of latent heat thermal energy storage units using carbon-fiber brushes: experiments and modeling.*" . Int J Heat Mass Transf 2003;46:4513–25.
- [35] Arun Kumar . S, A. Sekar, D.N. Siddhartha Jain, K.V. govinda " *Phase Change Materials for thermal control during spacecraft transportation.*" . System Integration Group, ISRO Satellite Centre.
- [36] Nasiru I, Fahad A, Saidur Rahman, Bekir S, Ahmet Z. Sahin " *Heat transfer enhancement of PCMs for thermal energy storage applications: A critical review.*" . Renewable and Sustainable Energy Reviews 74 (2017) 26–50.
- [37] M.M. Shapiro, D. Feldman, D. Hawes, D. Banu " *PCM thermal storage in wallboard.*" . Proceedings of the 12th Passive Solar Conference, Portland, 1987, pp. 45-48
- [38] F.Bruno, W. Swan, " *Testing of a PCM energy storage system for storage heating .*" . Proceedings of the world renewable energy congress, cologne, Germany, 2002.
- [39] Fabio Dal Margo, Haoxin Xu, Gioacchino, Alessandro Romagnoli " *Application of high temperature phase change materials for improved efficiency in waste-to-energy plants*" . Waste Management, June 2017, <https://doi.org/10.1016/j.wasman.2017.06.031>

Appendix



Project

First Saved	2 August 2017
Last Saved	15 September 2017
Product Version	17.2 Release
Save Project Before Solution	No
Save Project After Solution	No



Contents

- [Units](#)
- [Model \(R3\)](#)
 - [Geometry](#)
 - [Parts](#)
 - [Coordinate Systems](#)
 - [Connections](#)
 - [Contacts](#)
 - [Contact Regions](#)
 - [Mesh](#)
 - [Mesh Controls](#)
 - [Named Selections](#)

Units

TABLE 1

Unit System	Metric (mm, kg, N, s, mV, mA) Degrees rad/s Celsius
Angle	Degrees
Rotational Velocity	rad/s
Temperature	Celsius

Model (R3)

Geometry

TABLE 2
Model (R3) > Geometry

Object Name	<i>Geometry</i>
State	Fully Defined
Definition	
Source	C:\fluent\files to verify\new\importantfiles_files\dp0\FFF-18\DM\FFF-18.agdb
Type	DesignModeler
Length Unit	Meters
2D Behavior	Plane Stress
Bounding Box	
Length X	300, mm
Length Y	155, mm
Properties	
Volume	46500 mm ³
Surface Area(approx.)	46500 mm ²
Scale Factor Value	1,
Statistics	
Bodies	7
Active Bodies	7
Nodes	68109
Elements	66106
Mesh Metric	Aspect Ratio
Min	1
Max	22,097
Average	4,52872203430847
Standard Deviation	6,48733682933011
Basic Geometry Options	
Solid Bodies	Yes
Surface Bodies	Yes
Line Bodies	Yes
Parameters	Independent
Parameter Key	
Attributes	Yes
Attribute Key	
Named Selections	Yes
Named Selection Key	
Material Properties	Yes
Advanced Geometry Options	
Use Associativity	Yes
Coordinate Systems	Yes
Coordinate System Key	
Reader Mode Saves Updated File	No
Use Instances	Yes
Smart CAD Update	Yes
Compare Parts On Update	No
Attach File Via Temp File	Yes

Temporary Directory	C:\Users\jerolsoibam\AppData\Roaming\Ansys\v172
Analysis Type	2-D
Mixed Import Resolution	None
Decompose Disjoint Geometry	Yes
Enclosure and Symmetry Processing	No

TABLE 3
Model (R3) > Geometry > Parts

Object Name	<i>inpipe</i>	<i>fin1</i>	<i>fin2</i>	<i>fin3</i>	<i>pcm</i>	<i>outpipe</i>	<i>hotfluid</i>
State	Meshed						
Graphics Properties							
Visible	Yes						
Transparency	1						
Definition							
Suppressed	No						
Coordinate System	Default Coordinate System						
Thickness	1, mm						
Thickness Mode	Refresh on Update						
Behavior	None						
Reference Frame	Lagrangian						
Material							
Assignment							
Fluid/Solid	Defined By Geometry (Solid)						
Bounding Box							
Length X	300, mm				300, mm		
Length Y	5, mm	35, mm			70, mm	5, mm	75, mm
Properties							
Volume	1500, mm ³	105, mm ³			20685 mm ³	1500, mm ³	22500 mm ³
Centroid X	150, mm	76,5 mm	151,5 mm	226,5 mm	149,98 mm	150, mm	
Centroid Y	77,5 mm	97,5 mm			115,27 mm	152,5 mm	37,5 mm
Centroid Z	0, mm						
Surface Area (approx.)	1500, mm ²	105, mm ²			20685 mm ²	1500, mm ²	22500 mm ²
Statistics							
Nodes	6523	455	497	469	32661	1806	25698
Elements	5920	384	420	396	32163	1500	25323
Mesh Metric	Aspect Ratio						
Min	1,0001	1,0047	1,0003	1,0013	1		
Max	1,0143	1,2941	1,0655	1,1567	22,097	1	18,519
Average	1,01359826013514	1,09407994791667	1,01598380952381	1,06090555555556	6,75377756117266	1	2,89801725309005
Standard Deviation	1,86468282398219E-03	6,30252739638752E-02	,010021684115811	3,01751506357872E-02	7,42430980639644	0	5,16838621853446
CAD Attributes							
DMSheetThickness	0						

Coordinate Systems

TABLE 4
Model (R3) > Coordinate Systems > Coordinate System

Object Name	<i>Global Coordinate System</i>
State	Fully Defined
Definition	
Type	Cartesian
Coordinate System ID	0,
Origin	
Origin X	0, mm
Origin Y	0, mm
Directional Vectors	
X Axis Data	[1, 0,]
Y Axis Data	[0, 1,]

Connections

TABLE 5
Model (R3) > Connections

Object Name	<i>Connections</i>
State	Fully Defined
Auto Detection	
Generate Automatic Connection On Refresh	Yes
Transparency	
Enabled	Yes

TABLE 6
Model (R3) > Connections > Contacts

Object Name	Contacts
State	Fully Defined
Definition	
Connection Type	Contact
Scope	
Scoping Method	Geometry Selection
Geometry	All Bodies
Auto Detection	
Tolerance Type	Slider
Tolerance Slider	0,
Tolerance Value	0,84419 mm
Use Range	No
Edge/Edge	Yes
Priority	Include All
Group By	Bodies
Search Across	Bodies
Statistics	
Connections	9
Active Connections	9

TABLE 7
Model (R3) > Connections > Contacts > Contact Regions

Object Name	<i>inpipefin1</i>	<i>inpipefin2</i>	<i>inpipefin3</i>	<i>inpipepcm</i>	<i>inpipehotfluid</i>	<i>fin1pcm</i>	<i>fin2pcm</i>	<i>fin3pcm</i>	<i>pcmoutpipe</i>
State	Fully Defined								
Scope									
Scoping Method	Geometry Selection								
Contact	1 Edge				3 Edges			1 Edge	
Target	1 Edge		4 Edges		1 Edge	3 Edges		1 Edge	
Contact Bodies	inpipe					fin1	fin2	fin3	pcm
Target Bodies	fin1	fin2	fin3	pcm	hotfluid	pcm		outpipe	

Mesh

TABLE 8
Model (R3) > Mesh

Object Name	Mesh
State	Solved
Display	
Display Style	Body Color
Defaults	
Physics Preference	CFD
Solver Preference	Fluent
Relevance	0
Export Format	Standard
Shape Checking	CFD
Target Skewness	Program Controlled
Element Midside Nodes	Dropped
Sizing	
Size Function	Curvature
Relevance Center	Fine
Initial Size Seed	Active Assembly
Smoothing	High
Span Angle Center	Fine
Curvature Normal Angle	Default (18,0 °)
Min Size	1,0 mm
Max Face Size	1,0 mm
Growth Rate	Default (1,20)
Automatic Mesh Based Defeaturing	On
Defeature Size	Default (0,50 mm)
Minimum Edge Length	3,0 mm
Inflation	
Use Automatic Inflation	None
Inflation Option	First Layer Thickness
First Layer Height	5,4e-004 mm
Maximum Layers	10
Growth Rate	1,02
Inflation Algorithm	Pre
View Advanced Options	Yes
Collision Avoidance	Layer Compression
Fix First Layer	No
Gap Factor	0,5
Maximum Height over Base	1
Growth Rate Type	Geometric
Maximum Angle	140,0 °
Fillet Ratio	1

Use Post Smoothing	Yes
Smoothing Iterations	5
Assembly Meshing	
Method	None
Advanced	
Number of CPUs for Parallel Part Meshing	Program Controlled
Straight Sided Elements	
Number of Retries	0
Rigid Body Behavior	Dimensionally Reduced
Mesh Morphing	Disabled
Triangle Surface Mesher	Program Controlled
Topology Checking	No
Use Sheet Thickness for Pinch	No
Pinch Tolerance	Default (0,90 mm)
Generate Pinch on Refresh	No
Sheet Loop Removal	No
Statistics	
Nodes	68109
Elements	66106
Mesh Metric	Aspect Ratio
Min	1,
Max	22,097
Average	4,5287
Standard Deviation	6,4873

TABLE 9
Model (R3) > Mesh > Mesh Controls

Object Name	<i>Face Sizing</i>	<i>Inflation</i>	<i>Inflation 2</i>	<i>Face Meshing</i>
State	Fully Defined			
Scope				
Scoping Method	Geometry Selection			
Geometry	4 Faces	1 Face	4 Faces	
Definition				
Suppressed	No			
Type	Element Size			
Element Size	0,5 mm			
Boundary Scoping Method	Geometry Selection			
Boundary	1 Edge		14 Edges	
Inflation Option	First Layer Thickness			
First Layer Height	5,4e-002 mm			
Maximum Layers	10	15		
Growth Rate	1,02			
Inflation Algorithm	Pre			
Mapped Mesh	Yes			
Method	Quadrilaterals			
Constrain Boundary	No			
Advanced				
Defeature Size	Default (0,25 mm)			
Size Function	Uniform			
Behavior	Soft			
Growth Rate	Default (1,20)			
Specified Sides				No Selection
Specified Corners				No Selection
Specified Ends				No Selection

Named Selections

TABLE 10
Model (R3) > Named Selections > Named Selections

Object Name	<i>hotfluid</i>	<i>inpipe</i>	<i>pcm</i>	<i>fin1</i>	<i>fin2</i>	<i>fin3</i>	<i>outpipe</i>	<i>axis</i>	<i>inlet</i>	<i>outlet</i>	<i>wall1</i>
State	Fully Defined										
Scope											
Scoping Method	Geometry Selection										
Geometry	1 Face							1 Edge			
Definition											
Send to Solver	Yes										
Visible	Yes										
Program Controlled Inflation	Exclude										
Statistics											
Type	Manual										
Total Selection	1 Face							1 Edge			
Surface Area	22500 mm ²	1500, mm ²	20685 mm ²	105, mm ²	1500, mm ²						
Suppressed	0										
Used by Mesh Worksheet	No										
Length								300, mm	75, mm	70, mm	

TABLE 11
Model (R3) > Named Selections > Named Selections

Object Name	wal/2
State	Fully Defined
Scope	
Scoping Method	Geometry Selection
Geometry	1 Edge
Definition	
Send to Solver	Yes
Visible	Yes
Program Controlled Inflation	Exclude
Statistics	
Type	Manual
Total Selection	1 Edge
Length	70, mm
Suppressed	0
Used by Mesh Worksheet	No